JOC The Journal of Organic Chemistry

Article

Donor-Acceptor #-Conjugated Enamines: Functional Group Compatible Synthesis from Amides and Their Photoabsorption and Photoluminescence Properties

Atsushi Tahara, Ikumi Kitahara, Daichi Sakata, Yoichiro Kuninobu, and Hideo Nagashima

J. Org. Chem., **Just Accepted Manuscript** • DOI: 10.1021/acs.joc.9b02267 • Publication Date (Web): 28 Oct 2019

Just Accepted

is published by the American Chemical Society. 1155 Sixteenth Street N.W., Washington, DC 20036

(1) Title

Donor-Acceptor π-Conjugated Enamines: Functional Group Compatible Synthesis from Amides and Their Photoabsorption and Photoluminescence Properties

(2) Authors' names and addresses

Atsushi Tahara,[†] Ikumi Kitahara,[‡] Daichi Sakata,[‡] Yoichiro Kuninobu,[†,‡] Hideo Nagashima.[†,‡,*]

[†] Institute for Materials Chemistry and Engineering, and [‡]Interdisciplinary Graduate School of Engineering Sciences, Kyushu University, Kasuga, Fukuoka 816-8580, Japan.

(3) Corresponding author's e-mail address

*E-mail: nagasima@cm.kyushu-u.ac.jp

(4) Table of Contents/Abstract Graphic

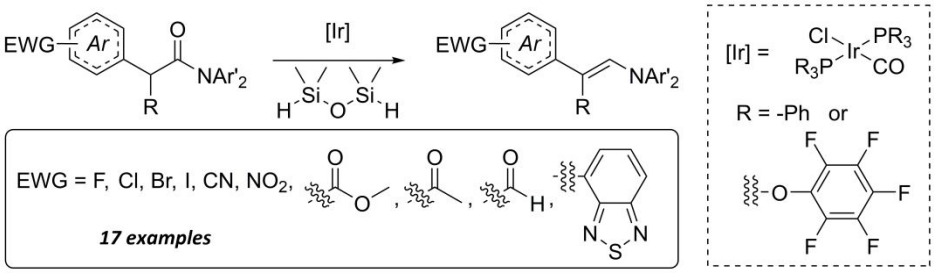

(5) Abstract

High functional group compatibility of iridium-catalyzed synthesis of enamines from amides and 1,1,3,3-tetramethyldisiloxane (TMDS) realized facile access of a series of Donor (D)-π-Acceptor (A) conjugated enamines, in which enamine behaves as a donor functional group. The amide precursors containing reducible functional groups, such as halogen, carbonyl, and nitro groups, underwent reaction with TMDS to give the corresponding enamines in high yields. In most cases, chemoselective hydrosilane reduction of the amide group occurred while other reducible groups remained intact. Absorption and emission properties including solvatochromic behavior for the resulting D-π-A conjugated enamines were determined using UV-visible and fluorescent spectra, which provided an understanding of the donor properties of the CH=CHNPh$_2$ group and photofunctional properties of the D-π-A conjugated enamines as a fluorescent dye. Maximum absorption wavelength (λ_{abs}) of *p*-

$ZC_6H_4CH{=}CHNPh_2$ was predictable from λ_{abs} of p-$ZC_6H_4NPh_2$, which was supported by DFT calculations. Some of the D-π-A conjugated enamines showed fluorescence with moderate fluorescence quantum yields (Φ_{fl}). Of interest are unusually emissive π-conjugated enamines containing a nitro group, which generally behaves as strong quenchers of fluorescence. Additive effect of $B(C_6F_5)_3$ resulted in significant red-shifts of λ_{abs} and λ_{fl}. In some cases, high Φ_{fl} was observed in the solution state.

(6) Introduction

Enamines have been recognized as a unique synthetic equivalent to enolates since the first report by Stork and coworkers.[1] While condensation of ketones or aldehydes with secondary amines has been used to produce enamines,[1a,1e] recent progress in transition metal-catalyzed reactions has provided several other alternative synthetic routes.[2] Among them, iridium-catalyzed reaction of tertiary amides with 1,1,3,3-tetramethyldisiloxane (TMDS) is a unique method for preparation of aldenamines with extremely high catalytic efficiency and excellent functional group compatibility.[3] The reaction involves two elementary steps, hydrosilylation of the C=O group in amides and subsequent elimination of a silanol from the resulting silylhemiaminal. In most cases, these two elementary reactions occur spontaneously.

Amides are less likely than other carbonyl groups, such as ketones and esters, to undergo hydride reduction.[4,5] As a consequence, selective reduction of amide groups is difficult when these reducible functional groups exist in the same molecule.[4,5e,6] The iridium-catalyzed reaction of tertiary amides with TMDS is of particular interest because the reaction is tolerant of ketone and ester groups to prepare easily the corresponding functionalized aldenamines from ketoamides and amide esters.[3a,3c]

A recent topic in enamine chemistry, which originated from materials science, is the excellent donor properties of π-conjugated enamines.[7] Since the report by Borsenberger and coworkers in 1997, hole-transport properties of several aldenamines conjugated to delocalized aromatic rings have been investigated.[7a] A recent contribution is facile preparation of π-conjugated aldenamines from *N,N*-diaryl-α-arylacetamide derivatives, which was achieved by the judicious choice of iridium catalysts.[3b] Compared with *N,N*-dialkylamides, *N,N*-diarylamides possess lower reactivity toward reaction with TMDS, and are more difficult to convert into the corresponding enamines when the catalyst $IrCl(CO)(PPh_3)_2$ (**I**) was used. Improved catalysts, such as $IrCl(CO)[P(OC_6F_5)_3]_2$ (**II**), $IrCl(PPh_3)_3$, and a species generated *in situ* from $[IrCl(\eta^4\text{-1,5-cyclooctadiene})]_2$ and phosphorous ligands, actually provided a method for the synthesis of a series of π-conjugated

enamines.[3b,3c]

These results prompted further research. Donor-acceptor π-conjugated dyes (D-π-A molecules), in which electron-donating (D) and electron-accepting (A) functional groups are linked by π-conjugated systems, have attracted considerable attention, especially in relation to biocompatible fluorescent dye labels, sensitizers of organic solar cells, components of organic light-emitting diodes, and other applications.[8] Since π-conjugated enamines act as an excellent electron donor in organic electronics, they were of interest because of their ability to act as donor functional groups in D-π-A molecules, which has not yet been explored. The present approach described here involves the preparation of a series of π-conjugated enamines containing various acceptor functional groups, along with studies on their UV-visible absorption and emission. A problem to overcome during synthesis was the selective hydrosilylation/silanol elimination sequence during the iridium-catalyzed reaction of *N,N*-diaryl-α-arylacetamides with TMDS, which produces the π-conjugated enamine donor portion with the acceptor functional groups remaining intact. Enamine formation from amides essentially involves hydride reduction of a C=O group, while many acceptor functional groups are susceptible to hydride reduction.[3-6] However, the selective reaction was accomplished by a judicious choice of the iridium catalyst. The donor properties of π-

conjugated enamines were determined by examination of the UV-visible spectra of the D-π-A conjugated enamines associated with TD-DFT calculations, and by evaluating the D-π-A conjugated enamines as a fluorescent dye in the fluorescence spectra.

(7) Results and Discussion

Preparation of D-π-A conjugated enamines. The representative D-π-A conjugated enamines were *p*-$ZC_6H_4CH{=}CHNPh_2$ (**4**), and a series of enamine products with different electron-accepting Z groups were synthesized by iridium-catalyzed reaction of the corresponding tertiary amides, *p*-$ZC_6H_4CH_2CONPh_2$ (**2**), with TMDS. A general reaction procedure involved use of $IrCl(CO)(PPh_3)_2$ (**1X**, 0.05–0.25 mol%) and TMDS (2 equiv. to **2**) in toluene at room temperature for 2 to 24 h. Reaction proceeded through formation of silylhemiaminal intermediates (**3**). In some cases, **3** was a major product of this reaction, and conversion of **3** to **4** was accomplished with ease by heating at 60 °C. As described previously, the reaction of *N,N*-dialkylacetamides with TMDS was complete within 1 h with catalyst loadings as low as 0.001 mol%.[3a] In contrast, reaction of *N,N*-diaryl-α-arylacetamides was slower, even when using active iridium catalysts such as $IrCl(CO)[P(OC_6F_5)_3]_2$ (**1Y**) with higher catalyst loadings at higher temperature for longer reaction times.[3b] In both cases, *E*-

enamine was obtained selectively. Halogens, cyano, carbonyl, and nitro groups were selected as the acceptor Z groups. These functional groups have a lone pair of electrons for coordination to the iridium center, which possibly lowers the catalytic activity. Carbonyl and nitro groups are typical reducible functional groups for hydride reduction, and hydrosilane reduction of these functional groups is potentially competitive with the enamine syntheses.[3-6] In our previous papers, we reported selective reduction of amide groups with ester and ketone groups remaining unreacted.[3a,3c] However, nitro, cyano and formyl groups have not been examined yet.

Halogen atoms as acceptor A. Table 1 shows the results for conversion of amides [Z = F (**2b**), Cl (**2c**), Br (**2d**), and I (**2e**)] to the corresponding enamines **4b**–**4e**. Treatment of the amide **2b** containing F with TMDS at room temperature for 2 h using $IrCl(CO)(PPh_3)_2$ (**1X**, 0.05 mol%) resulted in >99% conversion of **2b** to give a mixture of the silylhemiaminal **3b** (85%) and the enamine **4b** (9%) (entry 1). Heating the reaction mixture at 60 °C for 1 h led to complete conversion of **3b** to **4b**, and **4b** was obtained in 91% isolated yield. The Cl analogue **2c** reacted with TMDS in a similar manner (entry 2), although the reaction was somewhat slower and the silylhemiaminal **3c** was obtained as a single primary product. Isolated yield of **4c** after heat treatment was 71%. Although reaction of the Br derivative **2d**

was slower than that of **2c**, as shown in entry 3, the situation was improved when the more reactive catalyst $IrCl(CO)[P(OC_6F_5)_3]_2$ (**1Y**, 0.03 mol%) was used.[3b] Reaction was complete in 2 h, and the desired compound **4d** was obtained in 82% isolated yield (entry 4). The iodide-substituted enamine **4e** was the most difficult to synthesize among **4b**–**4e**. After optimizing the reaction conditions, **2e** was converted to **4e** using 0.3 mol% of **1Y** (entry 6, 72% isolated yield after 6 h). No silylhemiaminal was detected.

Table 1. Reaction of haloamides 2b-2e with TMDS catalyzed by 1X or 1Y.[a]

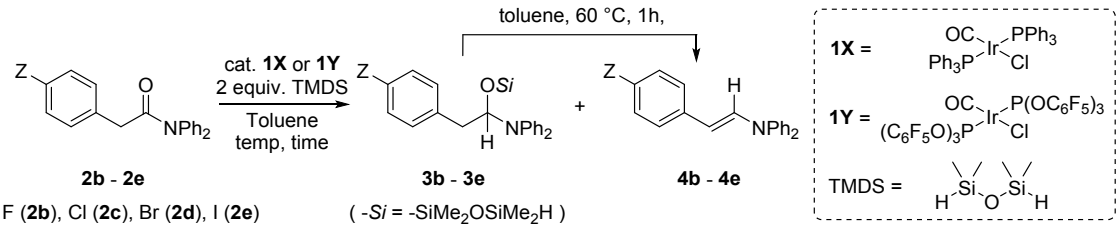

Entry	Substrate (Z =)	Cat. (mol%)	Temp. (°C)	Time (h)	Conv. of **2** (%)[b]	NMR Yield (%)[b]		Isolated yield of **4** after the heat treatment
						3	**4**	
1	**2b** (Z = F)	**1X** (0.05)	25	2	97	86	9	91
2	**2c** (Z = Cl)	**1X** (0.05)	25	4	95	95	0	71
3	**2d** (Z = Br)	**1X** (0.05)	25	4	48	49	0	--
4	**2d** (Z = Br)	**1Y** (0.03)	30	2	>99	16	83	82
5	**2e** (Z = I)	**1X** (0.05)	25	24	12	0	9	--
6	**2e** (Z = I)	**1Y** (0.30)	30	6	>99	0	92	72

[a]Reactions of the amide (1.00 mmol for entries 1-3 and 5, 0.50 mmol for entries 4 and 6) with TMDS (2.00 mmol for entries 1-3 and 5, 1.00 mmol for entries 4 and 6) were carried out in toluene (10 mL for entries 1-3 and 5, 5 mL for entries 4 and

6) in the presence of the catalyst **1X** or **1Y** (0.05 mol% ~0.3 mol%) under inert gas atmosphere. [b]Products existing in the reaction mixture. The yields were determined by ^{1}H NMR in the presence of anisole as an internal standard.

Palladium complexes often promote oxidative addition of aryl halides, *i.e.*, replacement of a C-X bond by a C-H bond in the presence of a hydrosilane.[9] Although the lower reactivity of **2d** and **2e** compared to **2b** and **2c** may be ascribed to oxidative addition of a C-X bond to a Vaska-type iridium complex, this possibility was excluded because oxidative addition of the C(sp^3)-X bond to **1X** is known, but that of a C(sp^2)-X bond has not been reported in the literature.[10] No C-X bond reduction by TMDS was actually observed in the reactions shown in Table 1. The lower reactivity of **2d** and **2e** instead was considered to be due to coordination of a lone pair of bromide or iodide to the catalytically active iridium center.

Benzothiadiazole as acceptor A. Benzothiadiazole (BTD) is a typical electron acceptor utilized for organic semiconductors,[11] having lone pairs on either nitrogen or sulfur atoms which potentially disturb the iridium-catalyzed reactions of the amide with TMDS. Thus, it was possible to assume that enamine formation could occur from **2f**, the amide containing BTD as an acceptor, though the reaction was disturbed by coordination of sulfur or nitrogen atoms in the BTD moiety. Reaction of **2f** to **4f** did not occur when **1X** was used as the catalyst. The use of more reactive catalyst **1Y** improved the situation, and treatment of **2f** with TMDS

in the presence of 0.5 mol% **1Y** gave **4f** as a single product with >99% NMR yield and 42% isolated yield (Scheme 1).

Scheme 1. Reaction of amide 2f bearing benzothiadiazole moiety with TMDS catalyzed by 1X or 1Y.

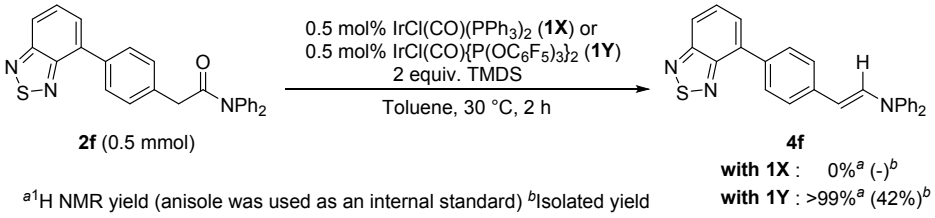

Cyano and alkoxycarbonyl groups as acceptor A. Cyano and alkoxycarbonyl groups undergo hydride reduction upon treatment with a strong reducing reagent such as $LiAlH_4$.[5,6] Their lone pairs potentially coordinate to the iridium center, slowing the reaction. While potential reduction of the Z groups in **2g** (Z = CN) and **2h** (Z = CO_2Me) was possible, these reactions occurred selectively only for the amide as shown in Table 2. No reaction occurred with **2g** in the presence of 0.05 mol% **1X** (entry 1). Use of **1Y** in higher catalyst loadings (0.5 mol%) at 30 °C led to complete conversion of **2g** after 1 h to form the corresponding silylhemiaminal quantitatively. After heat treatment, the desired enamine was isolated in 58% yield. Reaction of **2h** catalyzed by 0.1 mol% **1X** resulted in low conversion of **2h**, due to the low solubility

of amide **2h** in toluene (entry 3). Use of CH_2Cl_2 instead of toluene improved the conversion of **2h**, as shown in entry 4. Improvement also was made by using **1Y** as the catalyst in toluene, leading to >99% conversion of **2h** after 2 h, and a mixture of **3h** (32%) and **4h** (66%) was obtained.

Table 2. Reaction of amides bearing cyano (2g) or methoxycarbonyl (2h) groups with TMDS catalyzed by 1X or 1Y.[a]

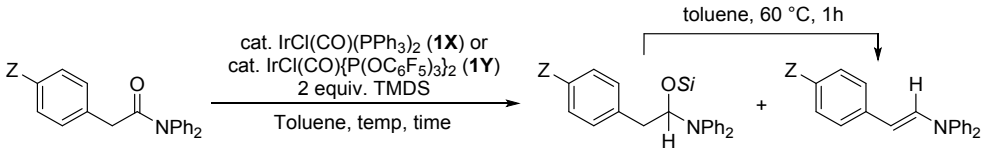

2g, 2h **3g, 3h** **4g, 4h**

Z = CN (**2g**), CO_2Me (**2h**) (-*Si* = $-SiMe_2OSiMe_2H$)

Entry	Substrate (Z =)	Cat. (mol%)	Temp. (°C)	Time (h)	Conv. of **2** (%)[b]	NMR Yield (%)[b]		Isolated yield of **4** after the heat treatment
						3	**4**	
1	**2g** (Z = CN)	**1X** (0.05)	25	24	0	0	0	--
2	**2g** (Z = CN)	**1Y** (0.5)	30	1	>99	>99	0	58
3	**2h** (Z = CO_2Me)	**1X** (0.1)	30	19	10	10	0	--
4[c]	**2h** (Z = CO_2Me)	**1X** (0.1)	30	19	>99	>99	0	61
5	**2h** (Z = CO_2Me)	**1Y** (0.1)	30	2	>99	32	66	--

[a] Reactions of the amide (0.50 mmol) with TMDS (1.0 mmol) were carried out in the presence of and the catalyst **1X** or **1Y** (0.05 mol% ~0.5 mol%) under inert gas atmosphere. Toluene was used as the solvent unless otherwise noted. [b] Products existing in the reaction mixture. The yields were determined by ^1H NMR in the presence of anisole as an internal standard. [c] CH_2Cl_2 was used as solvent.

Formyl and acetyl groups as acceptor A. Aldehydes and ketones are more susceptible than carboxylic acid derivatives to hydride reduction.[5,6] As a consequence, iridium-catalyzed enamine formation from amides and TMDS is accompanied by reduction of the C=O bond in formyl or acetyl groups as a side reaction. The lone pairs on the oxygen atom of the aldehydes and ketones have the potential to suppress the catalytic activity. This effect can be seen in Table 3, entries 1 and 3. The ketoamide **2i** (Z = COMe) did not react with TMDS with 0.01 mol% **1X**, whereas both amide and acetyl groups underwent reaction with TMDS to form enamines with a siloxy group **4j**, when **1Y** (0.05 mol%) was used as the catalyst. The situation was improved when the amount of **1X** was increased to 0.25 mol% (entry 2); selective preparation of ketoenamine **4i** was achieved after 2 h (>99% conversion of **2i**, >99% selectivity of the reaction, 68% isolated yield of **4i**). Aldehydes are more reactive than ketones toward hydride reduction. Reaction conditions were optimized based on the experimental results shown in entries 4–11. Similar to the reactions of **2i**, no reaction of **2k** occurred with a low catalyst loading (0.01 mol%, entry 4), whereas use of catalyst **1Y** resulted in hydrosilylation of both amide and formyl groups to form **3l** (entry 11). When the catalyst loading was increased to 0.1 mol% and the amount of TMDS was reduced from 2 equiv. per **2k** to 1 equiv., conversion of **2i** was moderate (entries 6-10). The optimized result

was use of 0.1 mol% of **1X** with 2 equiv. of TMDS to **2i** at room temperature for 2 h, which gave three products, **3k**, **4k**, and **3l**. After heat treatment of the mixture, all **3k** and **3l** were converted to **4k** and **4l**, respectively. Chromatographic separation from **4l** resulted in isolation of **4k** in 44% yield (entry 5).

Table 3. Reaction of amides bearing acetyl (2i) and formyl (2k) group with TMDS catalyzed by 1X or 1Y.[a]

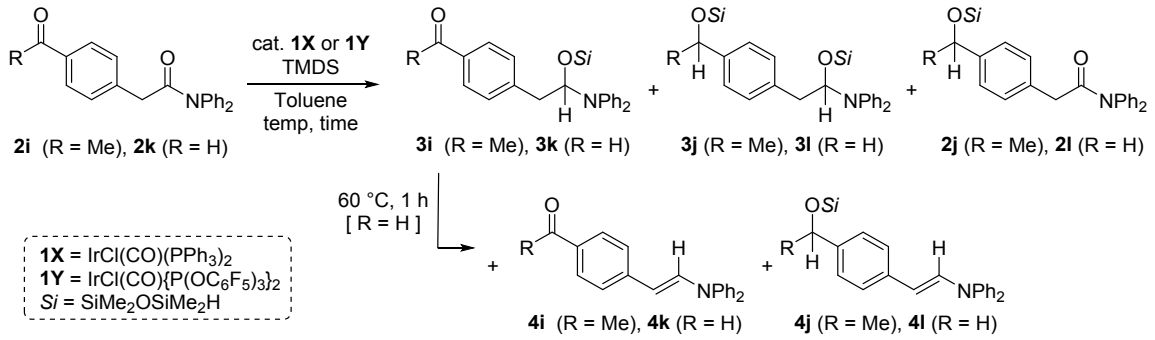

Entry	-R	Cat. (mol%)	Equiv. of TMDS	Temp. (°C)	Time (h)	Conv. of **2** (%)[b]	NMR yields (%)[b]					Isolated Yields of **4**
							[Desired product]		[Undesired product]			
							3i or **3k**	**4i** or **4k**	**3j** or **3l**	**4j** or **4l**	**2j** or **2l**	
1	-Me (**2i**)	**1X** (0.01)	2.0	30	19	0	-	-	-	-	-	-
2		**1X** (0.25)	2.0	30	2	>99	0	>99	0	0	0	68[c]
3		**1Y** (0.05)	2.0	30	0.5	>99	0	0	0	>99	0	-
4	-H (**2k**)	**1X** (0.01)	2.0	25	4	3	3	0	0	0	0	-
5		**1X** (0.1)	2.0	25	2	80	67	0	12	0	1	44[d]
6		**1X** (0.1)	1.3	25	4	57	37	0	7	0	6	-

7		**1X** (0.1)	1.1	25	4	56	45	0	4	0	3	-
8		**1X** (0.1)	1.0	25	4	63	41	0	8	0	5	-
9		**1X** (0.2)	1.0	25	4	79	48	16	10	0	2	-
10		**1X** (0.1)	1.0	30	4	53	34	10	6	0	3	-
11		**1Y** (0.1)	2.0	25	4	>99	0	0	0	68	29	-

[a]Reactions of **2i** or **2k** (0.50 mmol) with TMDS (1.0 mmol) were carried out in toluene (5.0 mL) in the presence of the catalyst (0.01 mol% ~0.25 mol%) under an inert gas atmosphere. [b]Determined by ^{1}H NMR in the presence of anisole as an internal standard. [c]Isolated yield after short column chromatography. [d]A reaction mixture was subjected to heat treatment to convert **3k** to **4k**. The resulting product was purified by column chromatography to separate **4k** from byproducts.

NO_2 group as acceptor A. Nitro groups are not reduced with many hydride reagents, although they are easily converted to an NH_2 or NHOH group by catalytic reduction with hydrogen[12] or hydrosilanes,[13] or by reduction with Fe powder in acetic acid.[14] Nitro groups have lone pairs on the oxygen, which potentially coordinate to transition metals and reduce catalytic activity. The reaction of **2m** (Z = NO_2) with TMDS in the presence of 0.5 mol% **1Y** at room temperature resulted in quantitative conversion of **2m** after 2 h, while no reaction proceeded when **1X** was used as the catalyst. After heat treatment, **4m** was obtained as a single product in 61% isolated yield (Table 4).

Table 4. Synthesis of π-conjugated enamines containing a NO_2 group.[a]

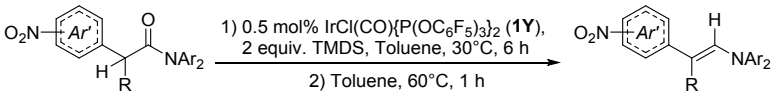

Amide 2, 5-8 **Enamine 4, 9-12**

entry	amide	enamine	yield (%)[b,c]
1	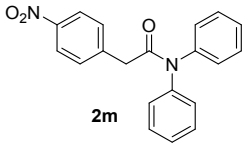 **2m**	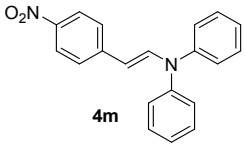 **4m**	>99% (61%)
2	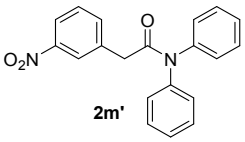 **2m'**	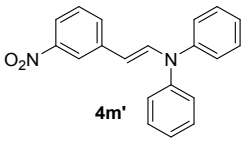 **4m'**	97% (73%)
3	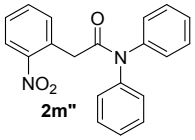 **2m"**	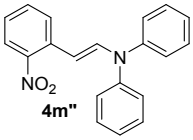 **4m"**	98% (75%)
4	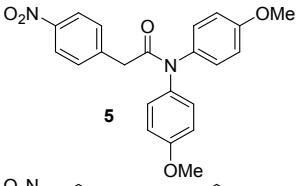 **5**	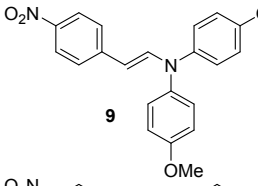 **9**	98% (79%)
5	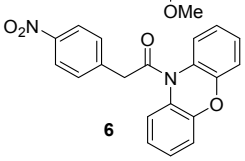 **6**	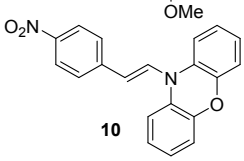 **10**	96% (40%)
6	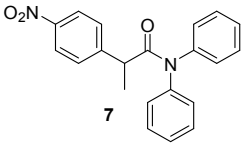 **7**	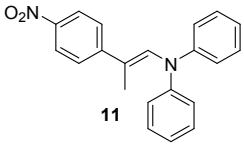 **11**	95% (58%)
7	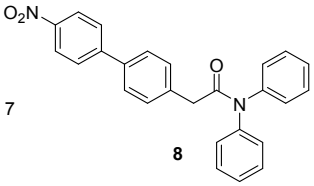 **8**	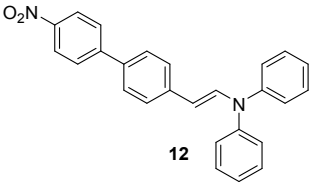 **12**	95% (59%)

[a]Reactions of amides (0.50 mmol) with TMDS (1.0 mmol) were conducted in toluene (5.0 mL) in the presence of **1Y** (0.5 mol%) under an inert gas atmosphere. [b]Determined by ^{1}H NMR in the presence of anisole as an internal standard. [c]Isolated yield in parentheses. Primary products obtained by the reactions of the amides are a mixture of the silylhemiaminal and the enamine, which were converted to the enamine by thermal treatment.

The ease of synthesizing enamine **4m** bearing a strongly electron-accepting NO_2 group prompted the preparation of a series of nitro enamines other than *p*-$O_2NC_6H_4CH{=}CHNPh_2$. The derivatization improved understanding of the donor properties of enamines in D-π-A molecules. The first point of the derivatization was the position change of the NO_2 group from the *para*- to the *meta*- (**4m'**) or *ortho*-position (**4m"**). The second point is alteration of the NPh_2 group to more electron-donating N(*p*-anisyl)$_2$ (**9**) or phenoxazinyl moiety (**10**). The third point is introduction of a methyl group on the C=C moiety at the β-position of the NPh_2 group (**11**). The fourth is elongation of the π-conjugate bridge by introduction of a C_6H_4 moiety (**12**). As summarized in Table 4, all of the derivatives were synthesized with the same procedure used for preparation of **4m**. Conversion of the starting materials and NMR yield of the product were >99%, but the isolated yields were lower because of losses during the purification process.

Absorption and emission spectra of 4. Properties of D-π-A enamines synthesized as described above were investigated by UV-visible spectroscopy with the aid of TD-DFT calculations. Table 5 shows experimentally obtained absorption wavelengths in toluene, in the solid state, and absorption wavelengths calculated by TD-DFT of compounds **4b-4i**, **4k**,

4m, **4m'**, **4m"**, and **9–12**. The calculated energy gap between the HOMO and LUMO of each compound also is provided. Solvent effects were not included in the TD-DFT data described in this table, indicating that the calculated values are those in gas phase. The calculated gas-phase absorption could be compared to those in non-polar solvents such as toluene. Experimental and calculated details are summarized in SI.

Table 5. Summary of experimentally obtained absorption and emission wavelengths (in toluene/solid state), calculated wavelengths (in gas phase) and HOMO-LUMO gap energies for enamines 4b–4m" and 9–12.

Entry	Compound	Absorption				Emission					
		Exp.[a]		Calcd. (gas phase)[b]		Exp. in toluene			Exp. in solid state		
		λ_{abs} [nm] in toluene (ε_{max} [cm^{-1}· M^{-1}])	λ_{abs} [nm] in solid state	λ_{calc} [nm]	$\Delta E_{HOMO-LUMO}$ [eV]	λ_{ex} [nm]	λ_{fl} [nm]	Φ_{fl}[d]	λ_{ex} [nm]	λ_{fl} [nm]	Φ_{fl}[d]
1	**4b**	309 (25,700), 332 (19,200)	325, 351	329, 355	3.99	310	386	<0.01[e]	325	–[f]	–[f]
2	**4c**	319 (22,800), 345 (24,600)	344, 363	331, 357	3.92	345	405	<0.01[e]	363	419	0.05
3	**4d**	319 (19,100), 347 (21,900)	337, 364	331, 359	3.90	350	405	<0.01[e]	364	422	<0.01
4	**4e**	309 (29,500), 349 (34,200)	350, 392	331, 360[c]	3.90[c]	350	408	<0.01[e]	392	437	<0.01
5	**4f**	316 (28,300), 345 (18,500), 426 (12,100)	326, 366, 470	338, 371, 547	2.57	425	552	0.61	470	624	0.07
6	**4g**	292 (33,700), 370 (31,700)	314, 390	256, 373	3.64	370	426	<0.01[e]	390	457	0.01
7	**4h**	315 (11,100), 370 (34,300)	307, 399	257, 378	3.61	370	432	<0.01[e]	399	474	0.06
8	**4i**	306 (10,600), 380 (30,200)	315, 394	285, 389	3.48	380	440	<0.01[e]	394	489	0.04

9	**4k**	290 (15,000), 392 (26,500)	307, 408	284, 392	3.41	390	450	<0.01[e]	408	511	0.05
10	**4m**	291 (14,500), 424 (21,700)	304, 487	299, 440	3.03	425	525	0.54	487	–[f]	–[f]
11	**4m'**	317 (20,500), 341 (27,000)	354, 548	346, 524	2.83	340	585	<0.01[e]	345	–[f]	–[f]
12	**4m"**	287 (13,500), 334 (10,300), 412 (3,400)	340, 362, 551	322, 346, 501	2.94	335	460	<0.01[e]	300	494	0.01
13	**9**	291 (20,200), 445 (19,500)	311, 466	299, 464	2.87	445	575	0.22	466	–[f]	–[f]
14	**10**	288 (11,900), 431 (17,000)	308, 421	280, 451	2.98	430	494	<0.01[e]	446	–[f]	–[f]
15	**11**	290 (20,800), 425 (12,800)	310, 474	306, 478	2.89	425	562	0.13	474	605	0.01
16	**12**	309 (23,800), 413 (26,000)	318, 447	361, 524	2.62	415	550	0.64	450	–[f]	–[f]

[a]Maximum absorption wavelengths of enamines in the solid state were described. Those for toluene solution in 10^{-5} M were also described with ε_{max}. [b]Calculation was performed under the condition described in experimental section unless otherwise noted. 12 excited states were calculated for TD-DFT. [c]SDD basis set was selected for I atom. [d]Absolute fluorescence quantum yield was described unless otherwise noted. [e]Determined by intensity relative to quinine sulfite (Φ_{fl} 0.55, ex. 350 nm) in 0.5 M sulfuric acid. [f]Not detected.

Two absorption peaks were observed at 300–500 nm for the compounds listed in the table, but the assignment of the peaks for the halogen derivatives **4b**–**4e** was different than those for the other compounds. In **4b** (Z = F), **4c** (Z = Cl), **4d** (Z = Br), and **4e** (Z = I), TD-DFT predicted two signals at *ca*. 330 and *ca*. 360 nm, which agree with those observed in UV-vis spectra in toluene. As shown in Fig. 1, the HOMO and LUMO of these compounds were π and π^*, respectively, in which orbitals are extensively delocalized in the molecules. The LUMO+1 of **4c** and **4d**, and LUMO+2 of **4b** and **4e,** consisted of π^* of the NPh_2 moiety

(π_2*), which has an energy level close to the LUMO. The two absorption maxima observed in the UV-vis spectra of **4b–4e** were ascribed to π-π* and π-π_2* transitions. In contrast, other compounds except **4f** provided a small and a large absorption peak around 260–340 nm and 370–500 nm. The former was a mixture of local transitions including π to π* of the NPh_2 moiety, whereas the latter was due to the π-π* transition. Although the reason is not clear, the TD-DFT calculations of **4f** did not reproduce the experimentally observed absorption spectra.

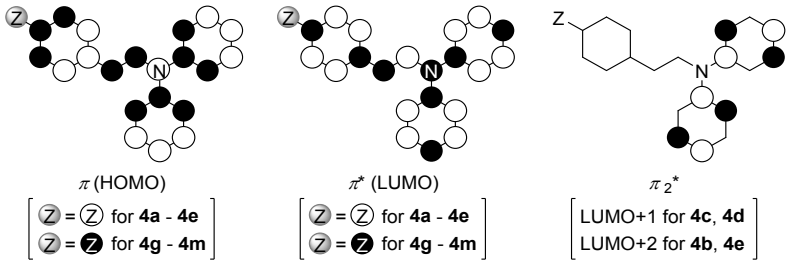

Figure 1. Molecular orbitals for enamines **4**.

Figure 2 shows plots of HOMO and LUMO energy levels of **4a–4m**. The HOMO and LUMO levels of each compound were lower than those calculated for **4a** having no substituent on the benzene ring. While the energy level change was relatively small in the halogen derivatives **4b–4e**, fewer of the compounds showed a lowering in the energy level of the HOMO (0.2–0.5 eV) and, more significantly, that of LUMO (0.6–1.5 eV). These

significant reductions in the energy level in the LUMO were due to the excellent π-acceptor nature of C≡N, C=O(OMe), C=O(Me), C=O(H), and NO_2, to which π-electrons in the enamines extensively delocalized. The effect of the NO_2 group was the most significant, which lowered the HOMO and LUMO levels of **4m** by 0.53 and 1.49 eV compared with those of **2a**. Similar effects of the NO_2 group were generally seen in the HOMO and LUMO levels of a series of nitro derivatives, **4m**, **4m'**, **4m''**, and **9–12** (see *2-1* in SI). The HOMO-LUMO gap of **4b–4e** was similar to that of **4a**, whereas that of the other compounds was smaller. This is in accord with the red-shift of the absorption of **4f–12** compared to that of **4a–4e**.

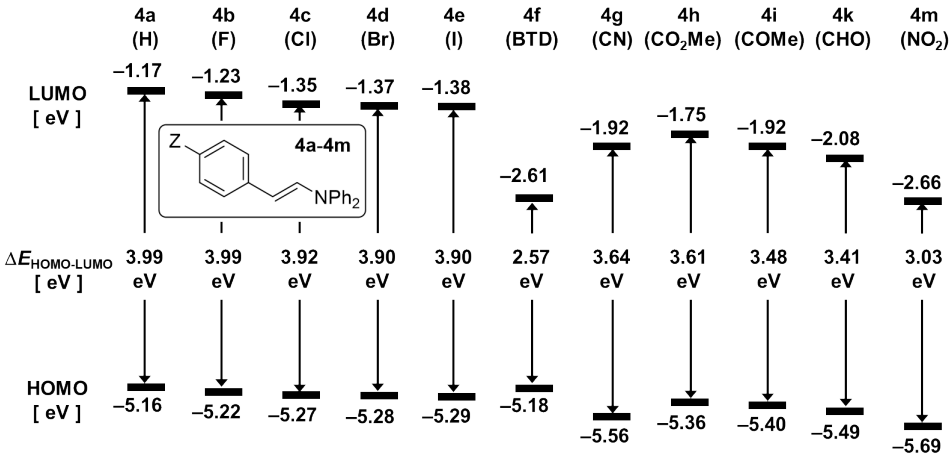

Figure 2. Calculated HOMO, LUMO and HOMO-LUMO gap ($\Delta E_{\text{HOMO-LUMO}}$) for enamines **4a~4m** [eV].

Fluorescence spectra of the compounds listed in Table 5 indicated that some of them were emissive. Relatively high quantum yields (Φ_{fl}) were available for **4f** (Z = BTD) and nitro derivatives, **4m**, **9**, **11**, and **12**. Of particular interest, is the remarkably high Φ_{fl} of the nitro derivatives. For example, **4m** and **12** produced strong fluorescence at 525 and 550 nm, with quantum yields reaching 54% and 64%, respectively. Nitroarenes are well known to be quenchers of fluorescence,[15] and only a few examples have been reported for highly emissive nitro compounds.[16,17] Almost all compounds in Table 5 did not produce fluorescence in the solid state. Although Φ_{fl} was lower than 10%, **4c** (Z = Cl), **4f–4k** (Z = BTD, CN, CO_2Me, COMe, and CHO), and nitro derivatives, **4m"**, and **11**, were emissive. The solvatochromic behavior of these compounds is discussed later.

Absorption spectra of *p*-$ZC_6H_4CH{=}CHNPh_2$, **4b–4m**, are predictable from those of *p*-$ZC_6H_4NPh_2$ having the same Z group. As shown in Fig. 3, maximum absorption wavelengths of **4a–4e** and **4g–4m** calculated by TD-DFT (λ_{calc}) linearly correlated with those of *p*-$ZC_6H_4NPh_2$ having the same Z group. Calculated absorption wavelength of *p*-$ZC_6H_4NPh_2$ was consistent with that obtained experimentally.[18] These are in accord with the additive rule of absorption spectra; λ_{calc} of *p*-$ZC_6H_4CH{=}CHNPh_2$ approximately corresponds to λ_{calc} of *p*-

$ZC_6H_4NPh_2$ plus 40 nm.[19] In contrast, emission behavior was complicated. Diphenylamino compounds, *p*-$ZC_6H_4NPh_2$ (Z = CN[18a] and CHO[18a,b]) reportedly showed fluorescence in THF at λ_{fl} of 421 and 465 nm with moderate quantum yields (0.29 and 0.36). In contrast, the corresponding enamine *p*-$ZC_6H_4CH{=}CHNPh_2$ [**4g** (Z = CN), **4k** (Z = CHO)] showed weak emission at λ_{fl} of 443 and 472 nm in THF. While *p*-$O_2NC_6H_4NPh_2$ is not fluorescent in MeCN,[18c] **4m** showed weak emission at 671 nm (*vide infra*).

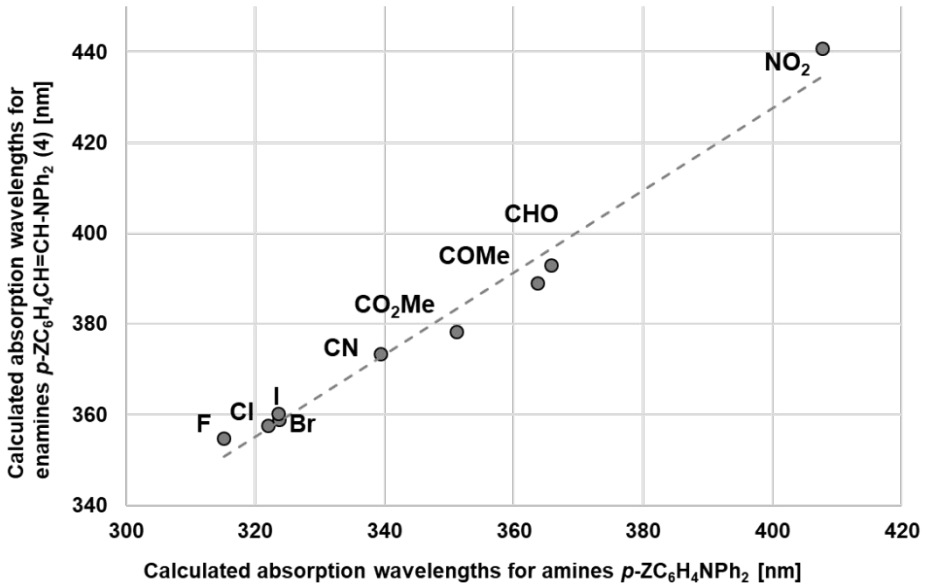

Figure 3. Plots of calculated absorption wavelengths for enamines **4** vs. those for the corresponding amines.

Solvatochromism in absorption and emission. Solvatochromisms typically observed in D-

π-A molecules, which are useful for understanding the ground as well as excited state properties of the molecules, have received considerable attention recently.[20] Figure 4 shows plots of λ_{abs} corresponding to π-π* transitions measured in six solvents: hexane, toluene, THF, $CHCl_3$, CH_2Cl_2, and DMF. From **4b** to **4g**, where Z = F, Cl, Br, I, BTD, and CN, a red shift of 5–8 nm was observed upon an increase in solvent polarity, indicating the appearance of positive solvatochromism. A relatively larger red shift of λ_{abs} (13–19 nm) was observed for carbonyl molecules, ester (**4h**), ketone (**4**i), and aldehyde (**4k**). The positive solvatochromism was most significant for the nitro derivative **4m**, which red-shifted more than 40 nm. In all cases, values of the red-shift had a linear relation with solvent polarity parameter $E_T(30)$[20a] (see *1-3* in SI).

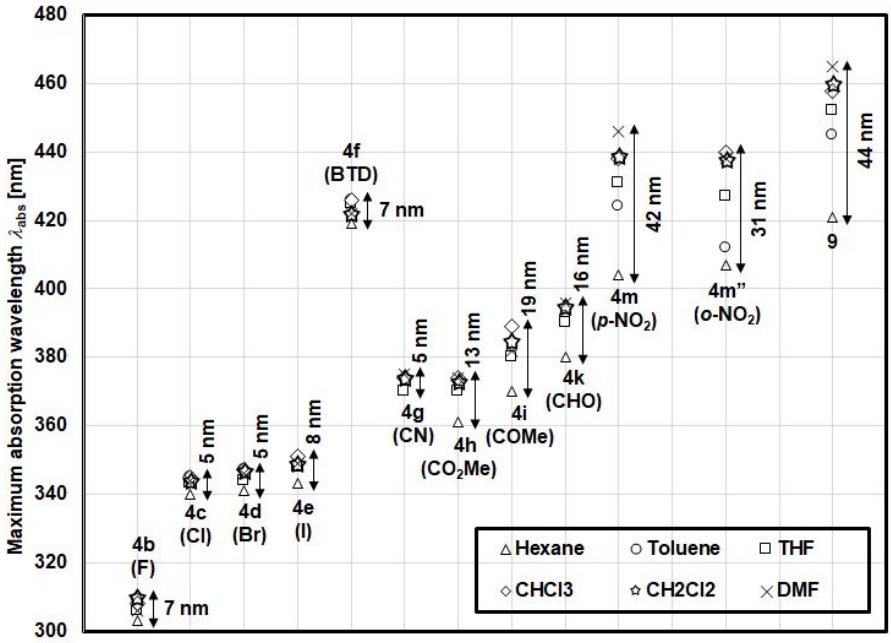

Figure 4. Plots of λ_{abs} for enamines **4b–4m, 4m"**, and **9** measured in six solvents (10^{-5} M solutions in hexane, toluene, THF, $CHCl_3$, CH_2Cl_2, DMF).

In general, positive solvatochromism is observed when the molecule in an excited state is better stabilized by polar solvents than that in the ground state.[20] Intramolecular charge transfer (ICT) of D-π-A compounds (Scheme 2) explains the present results. For compound **4**, an ionic resonance form **B** resulting from ICT (Scheme 2) contributed to stabilization of the excited states of **4**. Thus, contribution of **B** tends to be NO_2 > carbonyls > CN, BTD, halogen.

Scheme 2. Resonance structures of enamine 4.

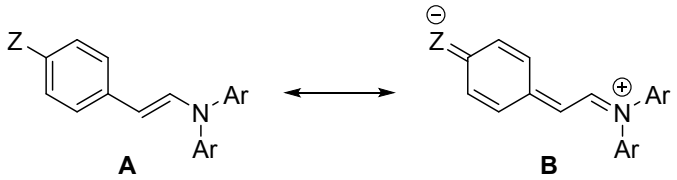

As described above, **4m** shows fluorescence in remarkably high quantum yield in toluene compared with those reported for other nitro compounds,[16b,17] making **4m** suitable for studying solvatochromic behavior in both absorption and emission spectra. The UV-vis and fluorescent spectra of **4m** were obtained in 12 aprotic solvents, of which $E_T(30)$ increased in the order: hexane < CCl_4 < toluene < 1,4-dioxane < THF < *o*-dimethoxybenzene (*o*-DMB) < $CHCl_3$ < CH_2Cl_2 < acetone < DMF < DMSO < MeCN. In addition, protic solvents EtOH and MeOH also were used for the measurements. Spectra in H_2O were not available due to lack of solubility of **4m**. Results are summarized in Table 6 and Figures 5 and 6. Relatively strong fluorescence ($\Phi_{fl} > 0.27$) was observed in CCl_4, toluene, 1,4-dioxane, THF and *o*-DMB with the fluorescence wavelength in the range of 508–595 nm. The quantum yield reached 0.69 in 1,4-dioxane. Although the quantum yield was low,[21] the longest emission wavelength of 671 nm was observed in MeCN. The spectrum in hexane gave two peaks and the quantum yield was lower than that in toluene. This may be explained by aggregation of **4m** in hexane like

prodan.[22] However, we do not have clear answer to this problem, because UV-vis absorption and fluorescence measurement of **4m** in hexane in two concentrations, 10^{-5} and 10^{-6} M, showed no difference in the peak ratio.

Table 6. Summary of experimentally obtained absorption and fluorescence wavelengths of 4m in various solvents.

Entry	Solvent	$E_T(30)$	λ_{abs} [nm (eV)][a]	ε_{max} [$cm^{-1}\cdot M^{-1}$]	λ_{fl} [nm (eV)][b]	Stokes shift [cm^{-1}]	Φ_{fl}[c]
1	Hexane	31.0	404 (3.069)	26,000	458 (2.707) 474 (2.616)	2918 3655	0.02
2	CCl_4	32.4	416 (2.981)	23,000	508 (2.441)	4353	0.27
3	Toluene	33.9	424 (2.925)	21,700	525 (2.361)	4537	0.54
4	1,4-Dioxane	36.0	425 (2.918)	26,300	546 (2.271)	5214	0.69
5	THF	37.4	431 (2.877)	30,200	568 (2.183)	5596	0.65
6	*o*-Dimethoxybenzene	38.4	441 (2.812)	11,400	595 (2.084)	5869	0.38
7	$CHCl_3$	39.1	438 (2.831)	24,200	637 (1.947)	7132	0.09
8	CH_2Cl_2	40.7	439 (2.825)	22,200	640 (1.937)	7154	0.05
9	Acetone	42.2	433 (2.864)	15,500	623 (1.990)	7043	0.08
10	DMF	43.2	446 (2.780)	22,400	655 (1.893)	7154	0.03
11	DMSO	45.1	452 (2.743)	21,000	669 (1.854)	7176	0.02
12	MeCN	45.6	434 (2.857)	34,800	671 (1.848)	8138	<0.01
13	EtOH	51.9	429 (2.890)	18,000	634 (1.956)	7537	<0.01
14	MeOH	55.4	430 (2.883)	14,300	643 (1.928)	7703	<0.01
15[d]	H_2O	62.8	–	–	–		–

[a]Maximum absorption wavelengths of **4m** in various solvent at 1.0×10^{-5} M were described [nm and eV in the parentheses].

[b]Maximum fluorescence wavelengths of **4m** in various solvent at 1.0×10^{-6} M were described [nm and eV in the parentheses].

[c]Absolute fluorescence quantum yield was described. [d]The data was not available due to lack of solubility of **4m** in H_2O.

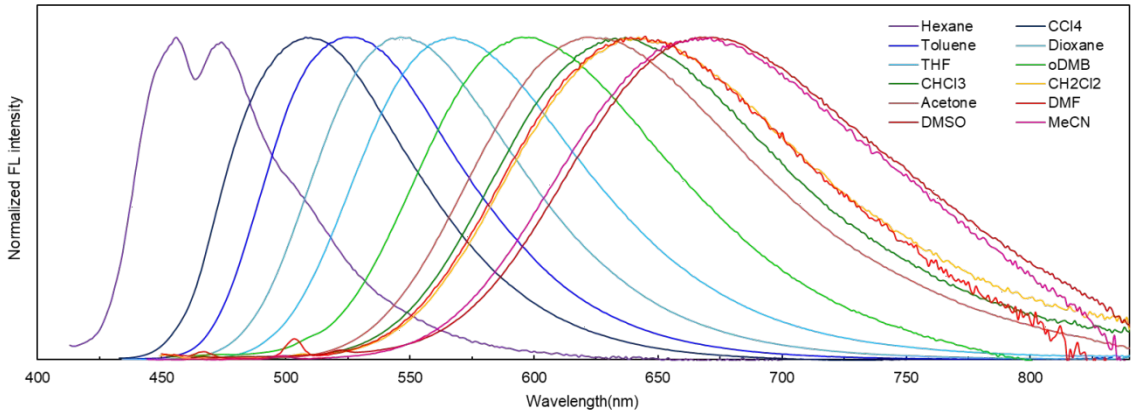

Figure 5. Emission spectra of **4m** obtained in various solvents. (Those for ROH were omitted for clarity. See Figure S57(f) in SI for complete spectra).

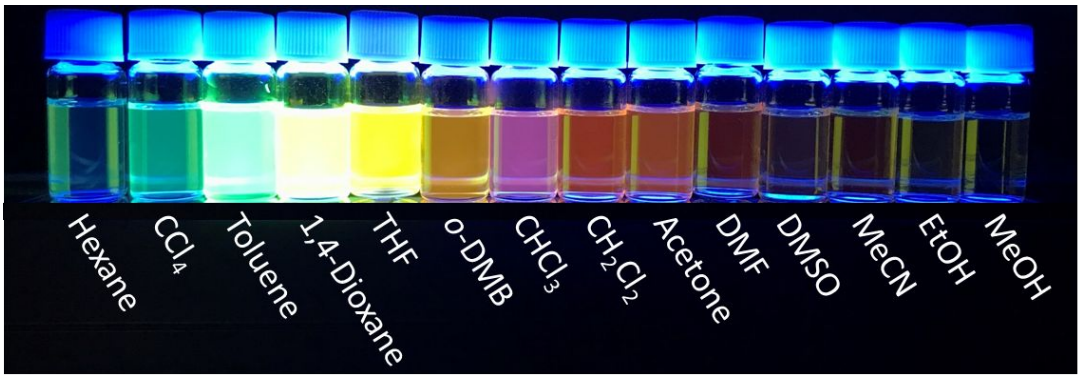

Figure 6. A series of solutions of **4m** in various solvents under UV light (365 nm)

A recent study on solvatochromism by Mennucci and coworkers involved the analysis of

solvatochromic behavior in solvents with different solvent polarity by solvent-induced shifts of absorption δ_{pol} (abs), fluorescent δ_{pol} (flu), and Stokes shift δ_{pol} (SS).[20b] To estimate solute-solvent hydrogen bonding, solvent-induced shifts of absorption δ_{HB} (abs), fluorescent δ_{HB} (flu), and Stokes shift δ_{HB} (SS) also were proposed as parameters. Table 7 shows experimentally obtained δ_{pol} (abs), δ_{pol} (flu), and δ_{pol} (SS) data when the solvent polarity increased from dioxane to DMSO. The table also includes δ_{HB} (abs), δ_{HB} (flu), and δ_{HB} (SS) upon changing the solvent from DMSO to MeOH. The data are compared with those obtained by common ICT probes, 6-propionyl-2-dimethylamino naphthalene (PRODAN)[23] and 7-diethylamino-9,9-dimethyl-9H-fluorene-2-carbaldehyde (FR-0).[23] The δ_{pol} (abs) and δ_{pol} (flu) values of **4m** are larger than those of PRODAN and FR-0, whereas δ_{pol} (SS) is between those of PRODAN and FR-0. Different from the negative δ_{HB} (abs) and δ_{HB} (flu) values of PRODAN and FR-0, those of **4m** are positive, while δ_{HB} (SS) of **4m** is smaller than δ_{HB} (SS) of PRODAN and FR-0. These indicate that **4m** behaves as a typical ICT probe in common organic solvents, but hydrogen bonding between **4m** and aprotic solvents does not provide a large effect on solvatochromic properties.

Table 7. Experimentally obtained solvent-induced shifts on absorption and emission energies (eV) and Stokes shift (cm^{-1}) for 4m.

compound	δ_{pol} (Dioxane-DMSO) (upper) δ_{HB} (DMSO-MeOH) (lower)		
	Absorption [eV]	Emission [eV]	Stokes shift [cm^{-1}]
4m	-0.18	-0.42	1962
	+0.14	+0.07	527
Prodan[23]	-0.11	-0.25	1161
	-0.06	-0.22	1339
FR-0[23]	-0.03	-0.38	2804
	-0.02	-0.20	1485

The solvatochromism of **4m** and other nitro derivatives was categorized into three classes: large shift (> 30 nm; **4m**, **4m”**, **9**), medium (10–20 nm; **10**, **11**), and small (< 10 nm; **4m’**, **12**). Despite the large red-shift, the absorption coefficient of **4m”** corresponding to the π-π* transition is small, due to the steric repulsion between the ortho-NO_2 group and the enamino group, which disturbs the NO_2 group coplanar with the benzene ring conjugated with the enamino group. The large shift is ascribed to a contribution of resonance form **B**, whereas the small red shift is explained by a factor that reduces the contribution of **B**. Among the two compounds showing small shifts, the *m*-nitroenamine **4m’** in the solid state showed two absorptions at 354 and 548 nm, which were in accord with the spectrum obtained by TD-

DFT calculations. The 548 nm absorption was missing in the solution state spectra, due to the π-π* transition being forbidden. That observed for **12** was due to an extra C_6H_4 ring between the nitro and enamino groups compared with **4m**, which does not provide a stable resonance form.

Lewis acid effects on absorption and emission. Three research groups recently published papers showing that addition of Lewis acidic molecules to non-emissive dye resulted in strong fluorescence.[24] The dyes used contain D-π-A structures, and the Lewis acidic additive coordinates to a functional group in the acceptor-induced red-shift of absorption and exhibit fluorescence in concentrated solutions and in solid states. A typical Lewis acid additive was $B(C_6F_5)_3$, while CN and CHO are useful Lewis basic functional groups (Scheme 3). The enamino-aldehyde **4k** was selected to investigate the absorption and fluorescent behavior in solution and solid states upon addition of $B(C_6F_5)_3$, which provided an impressive color change from yellow to red-violet. The UV-visible spectra of a mixture of **4k** and $B(C_6F_5)_3$ in $CHCl_3$ clearly demonstrated equilibrium with the adduct, *p*-$Ph_2NCH{=}CHC_6H_4CH{=}O{\cdot\cdot}B(C_6F_5)_3$ (**4k·B(C_6F_5)$_3$**). In dilute $CHCl_3$ solutions (10^{-5} M), two signals appeared at 392 and 525 nm, assigned to **4k** and the adduct, respectively. When the ratio of **4k** to $B(C_6F_5)_3$ was increased stepwise from 1:1 to 1:10, spectra changed with

isosbestic points and the peak due to the adduct increased in size (Fig. 7).

Scheme 3. Reaction of enamines 4 with $B(C_6F_5)_3$

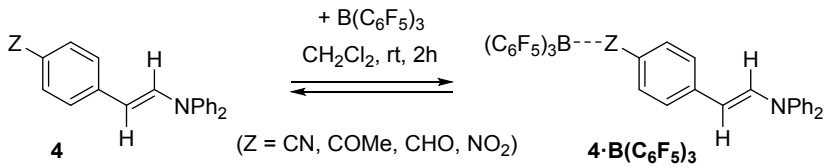

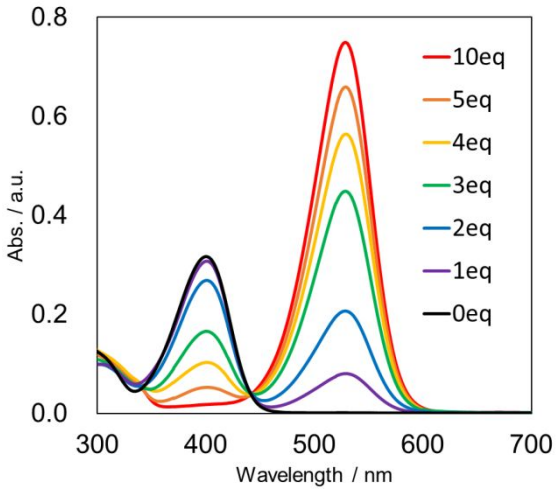

Figure 7. UV-vis absorption for a mixture of **4k** and $B(C_6F_5)_3$ in $CHCl_3$ at 10^{-5} M. The ratio of $B(C_6F_5)_3$ to **4k** were changed from 1 :1 to 10: 1.

Higher solute concentrations favored the formation of the adduct. The ^{1}H NMR spectrum

of **4k** in $CDCl_3$ at r.t. provided two CH protons in the enamino group at δ 5.58 (d, 1H) and 7.62 (d, 1H), two phenylene signals at δ 7.30 (d, 2H) and 7.72 (d 2H), and a formyl proton at δ 9.87 (s, 1H). In contact with $B(C_6F_5)_3$ (1 equiv. to **4k**), the phenylene signals appeared as four magnetically inequivalent doublets. Significant downfield shifts were observed for a *β*-proton of the enamino group and two of the phenylene protons. In contrast, the formyl signal was shifted upfield (see Fig. S43 in SI). These results are consistent with the complex *p*-$Ph_2NCH{=}CHC_6H_4CH{=}O{\cdot\cdot}B(C_6F_5)_3$. Since polar Lewis basic solvents, such as THF and DMF, disturbed the coordination of $B(C_6F_5)_3$ to the CHO group in **4k**, a solvatochromic study of the adduct was limited to four solvents, hexane (515 nm), toluene (529 nm), $CHCl_3$ (529 nm), and CH_2Cl_2 (533 nm), which showed positive absorption solvatochromism. In the solid state, a 1:1 mixture of **4k** and $\mathbf{B(C_6F_5)_3}$ showed a single absorption at 537 nm due to $\mathbf{4k{\cdot}B(C_6F_5)_3}$. Excitation of $\mathbf{4k{\cdot}B(C_6F_5)_3}$ around 520 nm resulted in photoluminescence at 569, 618, 642, and 683 nm in hexane, toluene, $CHCl_3$, and CH_2Cl_2, respectively, and at 785 nm in solid states. Quantum yields were 0.70, 0.22, 0.04, <0.01, and 0.03, respectively (see Table S4 in SI).

Other enamines, **4a**–**4j**, **4l**, and **4m**, were subjected to tests on the additive effect of $B(C_6F_5)_3$. Three enamines, **4g** (Z = CN), **4i** (Z = COMe), and **4m** (Z = NO_2), showed a

significant red-shift upon contact with $B(C_6F_5)_3$; absorption due to the adduct appeared at 429, 514, and 658 nm in toluene for **4g·B(C_6F_5)$_3$**, **4i·B(C_6F_5)$_3$**, and **4m·B(C_6F_5)$_3$**, which were red-shifted by 59, 134, and 234 nm compared with those of **4g**, **4i**, and **4m**, respectively. It is likely that $B(C_6F_5)_3$ was coordinated to a nitrogen atom of the CN group and an oxygen atom in the CHO, COMe, or NO_2 group. Coordination is strong in CN, COMe and CHO, and the absorption peaks due to the adduct were visible even in 10^{-5} M toluene solutions. In contrast, absorptions of **4m·B(C_6F_5)$_3$** were visible when using large amounts of $B(C_6F_5)_3$ (100 equiv. to the enamine). The DFT calculations provided optimized structures of $B(C_6F_5)_3$ adducts **4g·B(C_6F_5)$_3$**, **4i·B(C_6F_5)$_3$**, and **4m·B(C_6F_5)$_3$**. As expected, a boron atom of $B(C_6F_5)_3$ bonded with a nitrogen atom in a CN group or an oxygen atom of the CHO, COMe, or NO_2 group. To attempt to predict the absorption spectra of the adducts, TD-DFT calculations were performed; however, the program significantly underestimated absorption wavelength λ_{calc} compared with the corresponding experimental data, as shown in Table 8.

Table 8. Experimentally obtained absorption and emission wavelengths (in toluene/solid state) and calculated wavelengths (in gas phase) associated with HOMO-LUMO gap for several B(C_6F_5)$_3$ adducts of 4.[a]

En	Compound	Absorption	Emission

try		Exp.[b]		Calcd. (gas phase)[c]		Exp. in toluene			Exp. in solid state		
		λ_{abs} [nm] in toluene (Absorbance [a.u.])	λ_{abs} [nm] in solid state	λ_{abs} [nm]	$\Delta E_{HOMO-LUMO}$ [eV]	λ_{ex} [nm]	λ_{fl} [nm]	Φ_{fl}[d]	λ_{ex} [nm]	λ_{fl} [nm]	Φ_{fl}[d]
1	**4g·B(C_6F_5)$_3$**	429 (0.200)	431	414	3.24	429	502	0.04	431	580	0.02
2[e]	**4i·B(C_6F_5)$_3$**	514 (0.052)	524	467	2.80	514	587	0.97	524	613	0.01
3[f]	**4k·B(C_6F_5)$_3$**	529 (0.033)	537	461	2.81	529	612	0.25	537	785	0.03
4[g]	**4m·B(C_6F_5)$_3$**	658 (0.559)	668	552	2.31	658	–[h]	–[h]	668	–[h]	–[h]

[a]1equiv. of B(C_6F_5)$_3$ to enamine **4** was used unless otherwise noted. Since the adduct **4·B(C_6F_5)$_3$** was in equilibrium with uncoordinated enamine **4**, a peak due to the enamine appeared besides the peak ascribed to the adduct. Small absorbance is explained by this equilibrium. [b]Maximum absorption wavelengths of enamines in a toluene solution (10^{-5} M) / solid state are described. [c]Calculation was performed under the conditions described in experimental section unless otherwise noted. 30 excited states were calculated for TD-DFT. [d]Absolute fluorescence quantum yield was described. [e]Measured in toluene at 2.0×10^{-5} M. [f]Measured in toluene at 5.0×10^{-6} M. [g]100 equiv. of B(C_6F_5)$_3$ was used. [h]Not detected.

Of particular interest is the rationalization for the additive effect on absorption and emission properties. Figure 8 shows plots of absorption and fluorescence wavelength measured in toluene, which were dependent on the functional groups. Apparently, addition of B(C_6F_5)$_3$ to **4g**, **4i**, **4k**, and **4m** leads to a red-shift of λ_{abs} by 59–234 nm, and that to **4g**, **4i**, and **4k** gives rise to a red-shift of λ_{fl} by 76–162 nm, although the adduct **4m·B(C_6F_5)$_3$** showed no fluorescence wavelength below 950 nm. Whilst Φ_{fl} of **4g**, **4i**, and **4k** in toluene were smaller than 0.01, those of **4g·B(C_6F_5)$_3$**, **4i·B(C_6F_5)$_3$**, and **4k·B(C_6F_5)$_3$** in toluene were 0.04, 0.97,

and 0.25, respectively, which were significantly increased. The quantum yield of 0.97 for **4i·B(C_6F_5)$_3$** was the most impressive among them, but it is also notable that relatively high quantum yields were also observed for **4g·B(C_6F_5)$_3$** (0.11 in CH_2Cl_2) and **4k·B(C_6F_5)$_3$** (0.70 in hexane). Increase of quantum yields by addition of B(C_6F_5)$_3$ was not clearly visible in the solid state. Thus, coordination of B(C_6F_5)$_3$ to CN, CHO, COMe, and NO_2 likely enhances the acceptor property of these functional groups, changing the absorption and fluorescent properties of the D-π-A enamines.

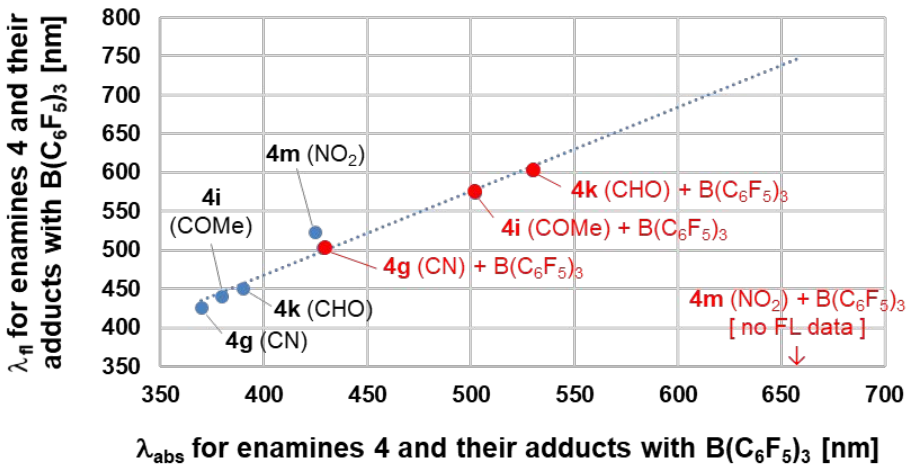

Figure 8. Plots of maximum absorption wavelength λ_{abs} for enamines **4g**, **4i**, **4k** and **4m**, and their adducts with B(C_6F_5)$_3$ in toluene vs. the corresponding maximum fluorescence wavelength λ_{fl}. λ_{abs} for **4m·B(C_6F_5)$_3$** appeared at 658 nm, while no fluorescence was observed below 950 nm.

(8) Conclusion and remarks

Iridium-catalyzed reactions of amides with TMDS have provided unique synthetic methods for enamines through silyl hemiaminal intermediates. The first step of the reaction is hydrosilylation of a C=O bond in the amide; this step also can be achieved by other transition-metal catalysts. The resulting silylhemiaminal intermediates are usually unstable, and undergo further reduction involving C=O bond fission to afford amines. An intriguing feature of the iridium-catalyzed reaction is that further reaction of the silylhemiaminal induces elimination of silanol to give enamines. In some cases involving an intermediate that forms π-conjugated enamines, silylhemiaminal is stable enough to isolate, to obtain spectroscopy on, and to use as synthetic intermediates for further transformations.[25]

Another intriguing feature of iridium-catalyzed enamine formation is high functional group compatibility; in particular, the selective reaction of amides with other carbonyl groups remains intact. The present report challenged selective synthesis of D-π-A conjugated enamines from *N,N*-diaryl-α-arylamides, in which acceptor groups, such as CHO, COMe, CO_2Me, CN and NO_2, are connected with the α-aryl group. Although π-conjugate enamine synthesis often requires more active iridium catalysts, which potentially increases the rate of side reactions that reduce the carbonyl group, selective enamine formation was achieved with

other reducible functional groups inside the molecule remaining unreacted.

Facile access to D-π-A conjugated enamines also promotes interest in their absorption and emission properties. The UV-vis and fluorescent spectra of a series of D-π-A conjugated enamines prepared using the selective enamine formation method provided information about the donor properties of arylenamines containing a $CH{=}CHNPh_2$ moiety: (1) The enamines prepared in this paper showed absorptions at 330~450 nm, which were reproducible by TD-DFT calculations. Maximum fluorescence wave length (λ_{fl}) was observed at 380~590 nm. (2) Maximum absorption wavelength (λ_{abs}) of *p*-$ZC_6H_4CH{=}CHNPh_2$ was predictable, which was ca. 40 nm red-shifted from λ_{abs} of the corresponding *p*-$ZC_6H_4NPh_2$. (3) Measurement of fluorescence spectra in toluene showed several compounds to be emissive. The quantum yields (Φ_{fl}) were moderate (0.13~0.64). Weak emission was observed in the solid states. (4) Positive solvatochromism was observed for both absorption and emission spectra. (5) While the nitro group generally acts as quencher of fluorescence, enamines containing nitro groups presented in this paper showed unusually strong emissions. In a typical example, Φ_{fl} of *p*-$O_2NC_6H_4CH{=}CHNPh_2$ in dioxane reached 0.69. (6) Addition of $B(C_6F_5)_3$ resulted in significant red shift of absorption and emission for the cyano, acetyl, formyl, and nitro derivatives. The coordination of $B(C_6F_5)_3$ was reversible,

and higher concentration of solutes favored for the adduct. (7) For cyano, acetyl and formyl adducts, the quantum yield of the adduct was higher than that of the enamine. For instance, Φ_{fl} of the $(C_6F_5)_3B$ adduct of *p*-MeC(=O)C_6H_4CH=CHNPh$_2$ in toluene reached 0.97 (Φ_{fl} of *p*-MeC(=O)C_6H_4CH=CHNPh$_2$ in toluene was below 0.01).

Comparison in absorption and emission properties with those of *N,N*-diphenylarylamines provides further interest. As shown in Scheme 4, Ar-NPh$_2$ can be prepared by cross-coupling of ArX with diphenylamine (the TOSOH-Buckwald-Hartwig amination),[26] whereas the enamines, ArCH=CHNPh$_2$, are accessible by two successive reactions, Hartwig's coupling of Ar-X with CH_2CONPh_2 anion[27] followed by the iridium-catalyzed reaction with TMDS. From the same precursor Ar-X, dyes with different absorption and fluorescent properties are readily available. The variety of absorption and fluorescent properties is increased by the Lewis acid effect of $B(C_6F_5)_3$, which was effective for enamines having a carbonyl or nitro group.

Scheme 4. Selective synthesis of Ar-NPh$_2$ and Ar-CH=CH-NPh$_2$ by cross-coupling reactions.

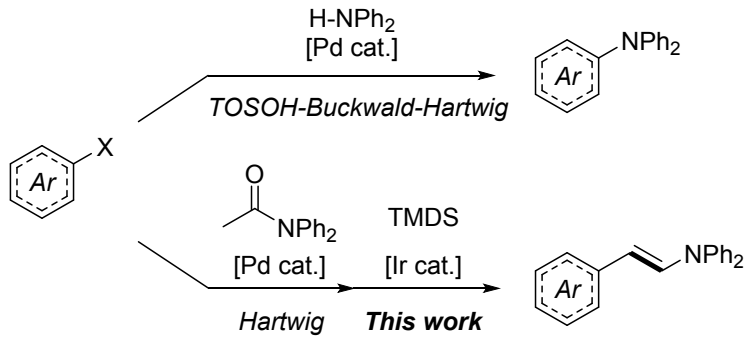

As photofunctional materials, such as fluorescent molecules, the D-π-A conjugated enamines need further enhancement to raise quantum yields of emission, in particular, in the solid state. Since various amide precursors for the present enamine formation are easily synthesized, molecules with better photofunctionality are likely to be discovered by further synthetic studies, as well as by prediction of properties using calculations. One of the examples for the expansion is synthesis of π-conjugated molecules containing dual D and/or dual A moieties. A preliminary experiment revealed that the D-π-A-π-D enamine **14** was easily prepared from the diamide **13** (Scheme 5). The resulting product **14** showed λ_{abs} at 464 and 484 nm and λ_{fl} at 571 and 670 nm in toluene and in the solid state, respectively. Compared with the D-π-A analogue **4f**, λ_{abs} and λ_{fl} were red-shifted by 14~46 nm, while small solvatochromic behavior (5 nm in both absorption and emission) was similar to that observed for **4f**. Fluorescence quantum yields of **14** in toluene were 0.29 and 0.07 in toluene

and in the solid state, respectively. Further studies seeking for excellent photofunctional molecules in this line are now underway.

Scheme 5. Synthesis of D-A-D enamine 14.

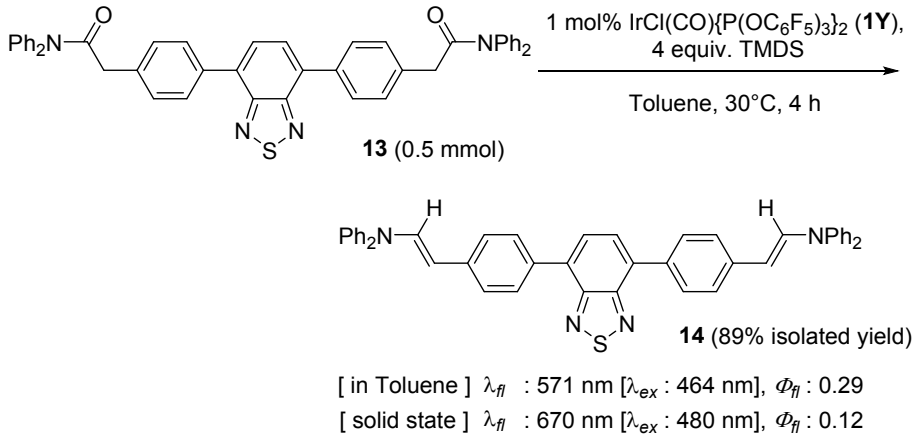

(9) Experimental Section

General Procedure. All manipulations were carried out under an argon or nitrogen atmosphere. ^{1}H, ^{13}C and ^{19}F NMR spectra were measured on JEOL ECA 400 (396 MHz) and ECA600 (600 MHz) spectrometers. Chemical shifts were given in parts per million relative to the solvent signal (^{1}H and ^{13}C NMR), whereas those for ^{19}F NMR were recorded based on

hexafluorobenzene ($\delta_F = -163.6$) as an external standard. IR spectra were taken on a JASCO FT/IR 4200 spectrometer. Melting points were measured on Stuart Scientific Melting Point Apparatus SMP3. HR-MS analyses were performed at the Analytical Center in Institute for Materials Chemistry and Engineering, Kyushu University. Deuterated solvents ($CDCl_3$) were purchased from Wako Pure Chemical Industries Ltd. and dried over activated MS4A (for $CDCl_3$) prior to use. Two reagents, 1,1,3,3-tetramethyldisiloxane (TMDS) and $B(C_6F_5)_3$, were purchased from AZmax Co. Ltd. and Wako Pure Chemical Industries Ltd., respectively, and purified by distillation (for TMDS) or sublimation (for $B(C_6F_5)_3$) prior to use. Dehydrated solvents [toluene, CH_2Cl_2, 1,4-dioxane] and solvents for UV-vis absorption and emission measurement [hexane, toluene, THF, $CHCl_3$, CH_2Cl_2, DMF] were purchased from Kanto Chemical Co. Ltd. or Wako Pure Chemical Industries Ltd., respectively, and used as received. Iridium catalysts $IrCl(CO)(PPh_3)_2$ (**1X**) and $IrCl(CO)\{P(OC_6F_5)_3\}_2$ (**1Y**) were prepared according to the reported procedure.[3] When the catalyst loading was small (0.05 ~ 0.3 mol%), a stock solution (0.5 M) in toluene was prepared, and used for the experiments. We checked CAS and found thirty compounds have the CAS numbers. However, no spectrum data for amide **2g** were given in the literature.[29] Other twenty-nine compounds were

reported in our patent.[30] Thus, we measured all of the compounds, HR-MS, NMR, IR, mp, and the data were described in experimental section. Actual charts are in SI.

General procedure for the preparation of amides 2b-2e, 2g, 2h, 2m, 2m', 2m", 5, 6, and 7. Synthesis of **2b-2e**, **2g**, **2h**, **2m**, **2m'**, **2m"**, **5**, **6**, and **7** was carried out by procedures similar to that reported for preparation of 2-phenyl-*N,N*-diphenylacetamide.[28] A general procedure was as follows: In a 200 ml of three-necked flask were placed carboxylic acid (5.00 ~ 32.0 mmol) and thionyl chloride (20.0~160 mmol, 5 molar equivalents to the carboxylic acid). A mixture was heated at 80 °C under reflux in oil bath for 2h. After the removal of the volatiles, a solution of secondary amine (4.20~26.0 mmol, 0.8 equiv. to the charged carboxylic acid) dissolved in 1,4-dioxane (11~70 ml) was added. The solution was heated at 100 °C under reflux in oil bath for 20 h. After cooling, 1M HCl aq. (2~14 ml) was added, and the mixture was extracted with CH_2Cl_2 (22~140 ml). Combined extracts were washed with sat. $NaHCO_3$ aq., and dried over $MgSO_4$. After filtration, the solution was concentrated *in vacuo*. The residue was purified by column chromatography (silica-gel, eluted by hexane: EtOAc = 10: 1) to afford the corresponding amide.

*2-(4-Fluorophenyl)-N,N-diphenylacetamide (**2b**)*.[30] From 2-(4-fluorophenyl)acetic acid (4.9 g, 32 mmol) and diphenylamine (4.4 g, 26 mmol), **2b** was obtained as white solid (7.3

g, 24 mmol, 92% in isolated yield). Mp : 78.5 ~ 79.6 °C. ^{1}H NMR (600 MHz, $CDCl_3$, –20 °C): δ 3.62 (s, 2H, -CH_2-), 6.95 (dd, J_{H-H} = 8.2 Hz, J_{H-F} = 8.9Hz, 2H, C_6H_4F), 7.06 (dd, J_{H-H} = 8.2 Hz, J_{H-F} = 4.1 Hz, 2H, C_6H_4F), 7.17 (t, J_{H-H} = 7.6 Hz, 1H, *p-Ph*), 7.19 (d, J_{H-H} = 7.6 Hz, 2H, *o-Ph*), 7.22 (d, J_{H-H} = 7.6 Hz, 2H, *o-Ph*), 7.31 (dd, J_{H-H} = 7.6, 7.6 Hz, 2H, *m-Ph*), 7.36 (t, J_{H-H} = 7.6 Hz, 1H, *p-Ph*), 7.40 (dd, J_{H-H} = 7.6, 7.6 Hz, 2H, *m-Ph*). ^{13}C{^{1}H} NMR (151 MHz, $CDCl_3$, –20 °C): δ 41.6, 115.6 (d, J_{C-F} = 20.2 Hz), 126.7, 126.7, 128.6, 129.2, 129.3 (d, J_{C-F} = 10.1 Hz), 130.2, 131.0, 131.0 (d, J_{C-F} = 8.7 Hz), 142.7, 142.7, 162.0 (d, J_{C-F} = 244.2 Hz), 171.5. ^{19}F NMR (565 MHz, $CDCl_3$, –20 °C): δ –116.1 (m). IR (ATR, cm^{-1}) : 1666 (ν_{CO}). HRMS-EI(+) (m/z) : [M]+ calcd for $C_{20}H_{16}NOF$, 305.1216; found, 305.1213. Actual charts are shown in Figures S5.

*2-(4-Chlorophenyl)-N,N-diphenylacetamide (**2c**)*.[30] From 2-(4-chlorophenyl)acetic acid (1.7 g, 10.0 mmol) and diphenylamine (1.4 g, 8.0 mmol), **2c** was obtained as white solid (2.1 g, 6.4 mmol, 80% in isolated yield). Mp : 110.7 ~ 111.1 °C. ^{1}H NMR (600 MHz, $CDCl_3$, –20 °C): δ 3.62 (s, 2H, -CH_2-), 7.05 (d, J_{H-H} = 8.3 Hz, 2H, C_6H_4Cl), 7.18 (t, J_{H-H} = 7.6 Hz, 1H, *p-Ph*), 7.19 (d, J_{H-H} = 7.6 Hz, 2H, *o-Ph*), 7.23 (d, J_{H-H} = 7.6 Hz, 2H, *o-Ph*), 7.25 (d, J_{H-H} = 8.3 Hz, 2H, C_6H_4Cl), 7.32 (dd, J_{H-H} = 7.6, 7.6 Hz, 2H, *m-Ph*), 7.37 (t, J_{H-H} = 7.6 Hz, 1H, *p-Ph*), 7.41 (dd, J = 7.6, 7.6 Hz, 2H, *m-Ph*). ^{13}C{^{1}H} NMR (151 MHz, $CDCl_3$, –20 °C): δ 41.5,

126.3, 126.4, 128.3, 128.5, 128.9, 129.0, 129.9, 130.5, 132.6, 133.4, 142.3, 142.4, 170.8. IR (ATR, cm^{-1}) : 1663 (ν_{CO}). HRMS-EI(+) (m/z) : [M]+ calcd for $C_{20}H_{16}NOCl$, 321.0920; found, 321.0921. Actual charts are shown in Figures S6.

*2-(4-Bromophenyl)-N,N-diphenylacetamide (**2d**)*.[30] From 2-(4-bromophenyl)acetic acid (2.2 g, 10.0 mmol) and diphenylamine (1.4 g, 8.0 mmol), **2d** was obtained as white solid (2.2 g, 6.0 mmol, 75% in isolated yield). Mp : 118 ~ 119 °C. ^{1}H NMR (600 MHz, $CDCl_3$, –20 °C): δ 3.60 (s, 2H, -CH_2-), 6.99 (d, J_{H-H} = 8.3 Hz, 2H, C_6H_4Br), 7.18 (1H, *p-Ph*, *overlapped with o-Ph*), 7.19 (d, J_{H-H} = 7.6 Hz, 2H, *o-Ph*), 7.23 (d, J_{H-H} = 7.6 Hz, 2H, *o-Ph*), 7.32 (dd, J_{H-H} = 7.6, 7.6 Hz, 2H, *m-Ph*), 7.38 (t, J_{H-H} = 7.6 Hz, 1H, *p-Ph*), 7.38 (d, J_{H-H} = 8.3 Hz, 2H, C_6H_4Br), 7.41 (dd, J_{H-H} = 7.6, 7.6 Hz, 2H, *m-Ph*). $^{13}C\{^1H\}$ NMR (151 MHz, $CDCl_3$, –20 °C): δ 41.5, 120.8, 126.3, 126.4, 128.3, 128.9, 129.0, 129.9, 130.9, 131.4, 133.9, 142.2, 142.3, 170.6. IR (ATR, cm^{-1}) : 1664 (ν_{CO}). HRMS-EI(+) (m/z) : [M]+ calcd for $C_{20}H_{16}NOBr$, 365.0415; found, 365.0417. Actual charts are shown in Figures S7.

*2-(4-Iodophenyl)-N,N-diphenylacetamide (**2e**)*.[30] From 2-(4-iodophenyl)acetic acid (2.6 g, 10.0 mmol) and diphenylamine (1.4 g, 8.0 mmol), **2e** was obtained as white solid (2.5 g, 6.0 mmol, 75% in isolated yield). Mp :125.4 ~ 126.4 °C.^{1}H NMR (600 MHz, $CDCl_3$, –20 °C): δ 3.59 (s, 2H, -CH_2-), 6.86 (d, J_{H-H} = 8.3 Hz, 2H, C_6H_4I), 7.18 (1H, *p-Ph*, *overlapped with o-*

Ph), 7.18 (d, J_{H-H} = 7.6 Hz, 2H, *o-Ph*), 7.22 (d, J_{H-H} = 7.6 Hz, 2H, *o-Ph*), 7.32 (dd, J_{H-H} = 7.6, 7.6 Hz, 2H, *m-Ph*), 7.37 (t, J_{H-H} = 7.6 Hz, 1H, *p-Ph*), 7.41 (dd, J_{H-H} = 7.6, 7.6 Hz, 2H, *m-Ph*), 7.58 (d, J_{H-H} = 8.3 Hz, 2H, C_6H_4I). $^{13}C\{^1H\}$ NMR (151 MHz, $CDCl_3$, –20 °C): δ 41.6, 92.5, 126.3, 126.4, 128.3, 128.9, 129.0, 129.9, 131.2, 134.6, 137.4, 142.3, 142.3, 170.6. IR (ATR, cm^{-1}) : 1662 (ν_{CO}). HRMS-EI(+) (m/z) : [M]+ calcd for $C_{20}H_{16}NOI$, 413.0277; found, 413.0278. Actual charts are shown in Figures S8.

*2-(4-Cyanophenyl)-N,N-diphenylacetamide (**2g**)*.[29] From 2-(4-cyanophenyl)acetic acid (2.6 g, 16.0 mmol) and diphenylamine (2.2 g, 13.0 mmol), **2g** was obtained as yellow solid (1.8 g, 5.4 mmol, 42% in isolated yield). Mp : 101 ~ 102 °C. ^1H NMR (600 MHz, $CDCl_3$, –20 °C): δ 3.71 (s, 2H, $-CH_2-$), 7.21 (1H, *p-Ph*, *overlapped with o-Ph*), 7.19 (d, J_{H-H} = 7.6 Hz, 2H, *o-Ph*), 7.22 (d, J_{H-H} = 7.6 Hz, 2H, *o-Ph*), 7.24 (d, J_{H-H} = 8.3 Hz, 2H, C_6H_4CN), 7.33 (dd, J_{H-H} = 7.6, 7.6 Hz, 2H, *m-Ph*), 7.39 (t, J_{H-H} = 7.6 Hz, 2H, *p-Ph*), 7.42 (dd, J_{H-H} = 7.6, 7.6 Hz, 2H, *m-Ph*), 7.57 (d, J_{H-H} = 8.3 Hz, 2H, C_6H_4CN). $^{13}C\{^1H\}$ NMR (151 MHz, $CDCl_3$, –20 °C): δ 42.1, 110.5, 119.1, 126.2, 126.6, 128.5, 128.8, 129.1, 130.0, 130.0, 132.2, 140.5, 142.0, 142.1, 169.8. IR (ATR, cm^{-1}) : 1663 (ν_{CO}), 2228 (ν_{CN}). Mp : 101 ~ 102 °C. HRMS-EI(+) (m/z) : [M]+ calcd for $C_{21}H_{16}N_2O$, 312.1263; found, 312.1262. Actual charts are shown in Figures S10.

2-{4-(Methoxycarbonyl)phenyl}-N,N-diphenylacetamide ***(2h)***. From 2-{4-(methoxycarbonyl)phenyl}acetic acid (1.0 g, 5.0 mmol) and diphenylamine (0.7 g, 4.2 mmol), **2h** was obtained as white solid (1.5 g, 3.6 mmol, 85% in isolated yield). Mp : 166 ~ 167 °C. ^{1}H NMR (600 MHz, $CDCl_3$, –20 °C): δ 3.72 (s, 2H, -CH_2-), 3.90 (s, 3H, -OCH_3), 7.16 (d, J_{H-H} = 7.6 Hz, 2H, *o-Ph*), 7.17 (d, J_{H-H} = 8.3 Hz, 2H, $C_6H_4CO_2CH_3$), 7.18 (1H, *p-Ph*, *overlapped with o-Ph*), 7.22 (d, J_{H-H} = 7.6 Hz, 2H, *o-Ph*), 7.32 (dd, J_{H-H} = 7.6, 7.6 Hz, 2H, *m-Ph*), 7.37 (t, J_{H-H} = 7.6 Hz, 1H, *p-Ph*), 7.39 (dd, J_{H-H} = 7.6, 7.6 Hz, 1H, *m-Ph*), 7.93 (d, J_{H-H} = 8.3 Hz, 2H, $C_6H_4CO_2CH_3$). ^{13}C{^{1}H} NMR (151 MHz, $CDCl_3$, –20 °C): δ 42.3, 52.4, 126.3, 126.5, 128.3, 128.5, 128.9, 129.1, 129.2, 129.7, 129.9, 140.3, 142.3, 142.3, 167.2, 170.5. IR (ATR, cm^{-1}) : 1676 (ν_{CONPh2}), 1709 (ν_{COOMe}). HRMS-EI(+) (m/z) : [M]+ calcd for $C_{22}H_{19}NO_3$, 345.1365; found, 345.1365. Actual charts are shown in Figures S11.

2-(4-Nitrophenyl)-N,N-diphenylacetamide ***(2m)***.[30] From 2-(4-nitrophenyl)acetic acid (5.8 g, 32.0 mmol) and diphenylamine (4.4 g, 26.0 mmol), **2m** was obtained as yellow solid (7.8 g, 23.0 mmol, 90% in isolated yield). Mp : 114.4 ~ 115.5 °C. ^{1}H NMR (600 MHz, $CDCl_3$, –20 °C): δ 3.76 (s, 2H, -CH_2-), 7.20 (t, J_{H-H} = 7.6 Hz, 1H, *p-Ph*), 7.21 (d, J_{H-H} = 7.6 Hz, 2H, *o-Ph*), 7.22 (d, J_{H-H} = 7.6 Hz, 2H, *o-Ph*), 7.31 (d, J_{H-H} = 8.3 Hz, 2H, $C_6H_4NO_2$), 7.33 (dd, J_{H-H} = 7.6, 7.6 Hz, 2H, *m-Ph*), 7.40 (t, J_{H-H} = 7.6 Hz, 1H, *p-Ph*), 7.43 (dd, J_{H-H} = 7.6, 7.6 Hz,

2H, *m-Ph*), 8.15 (d, J_{H-H} = 8.3 Hz, 2H, $C_6H_4NO_2$). $^{13}C\{^1H\}$ NMR (151 MHz, $CDCl_3$, –20 °C): δ 42.0, 123.7, 126.3, 126.6, 128.6, 128.9, 129.1, 130.1, 130.2, 142.0, 142.1, 142.7, 146.7, 169.7. IR (ATR, cm^{-1}) : 1662 (ν_{CO}). HRMS-EI(+) (m/z) : [M]+ calcd for $C_{20}H_{16}N_2O_3$, 332.1161; found, 332.1159. Actual charts are shown in Figures S14.

*2-(3-Nitrophenyl)-N,N-diphenylacetamide (**2m'**)*.[30] From 2-(3-nitrophenyl)acetic acid (2.9 g, 16.0 mmol) and diphenylamine (2.2 g, 13.0 mmol), **2m'** was obtained as pale brown solid (3.5 g, 11.6 mmol, 90% in isolated yield). Mp : 95.7 ~ 96.3 °C. ^1H NMR (600 MHz, $CDCl_3$, –20 °C): δ 3.75 (s, 2H, $-CH_2-$), 7.21 (t, J_{H-H} = 7.6 Hz, 1H, *p-Ph*), 7.24 (d, J_{H-H} = 7.6 Hz, 2H, *o-Ph*), 7.26 (d, J_{H-H} = 7.6 Hz, 2H, *o-Ph*), 7.33 (dd, J_{H-H} = 7.6, 7.6 Hz, 2H, *m-Ph*), 7.42 (t, J_{H-H} = 7.6 Hz, 1H, *p-Ph*), 7.44 (dd, J_{H-H} = 7.6, 7.6 Hz, 2H, *m-Ph*), 7.48 (dd, J_{H-H} = 8.3, 8.3 Hz, 1H, $C_6H_4NO_2$), 7.58 (d, J_{H-H} = 8.3 Hz, 1H, $C_6H_4NO_2$), 7.94 (s, 1H, $C_6H_4NO_2$), 8.12 (d, J_{H-H} = 8.3 Hz, 1H, $C_6H_4NO_2$). $^{13}C\{^1H\}$ NMR (151 MHz, $CDCl_3$, –20 °C): δ 41.6, 122.1, 124.5, 126.3, 126.6, 128.6, 128.8, 129.1, 129.4, 130.1, 135.9, 136.9, 142.0, 142.1, 147.9, 169.9. IR (ATR, cm^{-1}) : 1676 (ν_{CO}). HRMS-EI(+) (m/z) : [M]+ calcd for $C_{20}H_{16}N_2O_3$, 332.1161; found, 332.1159. Actual charts are shown in Figures S15.

*2-(2-Nitrophenyl)-N,N-diphenylacetamide (**2m"**)*.[30] From 2-(2-nitrophenyl)acetic acid (2.9 g, 16.0 mmol) and diphenylamine (2.2 g, 13.0 mmol), **2m"** was obtained as pale brown

crystal (1.5 g, 4.9 mmol, 38% in isolated yield). Mp: 160.3 ~ 160.6 °C. ^{1}H NMR (600 MHz, $CDCl_3$, –20 °C): δ 3.91 (s, 2H, -CH_2-), 7.17 (br, 1H, *p-Ph*), 7.29-7.32 (a mixture of signals, 4H, *o-Ph* and *m-Ph*), 7.31 (d, J_{H-H} = 7.6 Hz, 1H, $C_6H_4NO_2$), 7.40 (br, 1H, *p-Ph*), 7.44 (dd, J_{H-H} = 7.6, 7.6 Hz, 1H, $C_6H_4NO_2$), 7.47-7.51 (a mixture of signals, 4H, *o-Ph* and *m-Ph*), 7.58 (dd, J_{H-H} = 7.6, 7.6 Hz, 1H, $C_6H_4NO_2$), 8.14 (d, J_{H-H} = 7.6 Hz, 1H, $C_6H_4NO_2$). ^{13}C{^{1}H} NMR (151 MHz, $CDCl_3$, –20 °C): δ 41.9, 125.3, 126.3, 126.3, 128.4, 128.4, 128.9, 128.9, 130.1, 131.6, 133.8, 133.8, 142.2, 142.3, 148.2, 169.6. IR (ATR, cm^{-1}) : 1673 (ν_{CO}). HRMS-EI(+) (m/z) : [M]+ calcd for $C_{20}H_{16}N_2O_3$, 332.1161; found, 332.1160. Actual charts are shown in Figures S16.

*2-(4-Nitrophenyl)-N,N-di(4-methoxyphenyl)acetamide (**5**)*.[30] From 2-(4-nitrophenyl)acetic acid (1.45 g, 8.0 mmol) and di(4-methoxyphenyl)amine (1.5 g, 6.5 mmol), **5** was obtained as pale brown solid (1.7 g, 4.3 mmol, 66% in isolated yield). Mp: 81.3 ~ 82.6 °C. ^{1}H NMR (600 MHz, $CDCl_3$, –20 °C): δ 3.74 (s, 2H, -CH_2-), 3.76 (s, 3H, -OCH_3), 3.83 (s, 3H, -OCH_3), 6.83 (d, J_{H-H} = 8.9 Hz, 2H, C_6H_4OMe), 6.90 (d, J_{H-H} = 8.9 Hz, 2H, C_6H_4OMe), 7.11 (d, J_{H-H} = 8.9 Hz, 2H, C_6H_4OMe), 7.14 (d, J_{H-H} = 8.9 Hz, 2H, C_6H_4OMe), 7.31 (d, J_{H-H} = 8.3 Hz, 2H, $C_6H_4NO_2$), 8.14 (d, J_{H-H} = 8.3 Hz, 2H, $C_6H_4NO_2$). ^{13}C{^{1}H} NMR (151 MHz, $CDCl_3$, –20 °C): δ 41.7, 55.5, 55.7, 114.2, 114.9, 123.7, 127.3, 129.7, 130.2, 135.2, 135.2, 142.9, 146.7, 157.6,

159.0, 170.1. IR (ATR, cm^{-1}) : 1656 (ν_{CO}). HRMS-EI(+) (m/z) : [M]+ calcd for $C_{22}H_{20}N_2O_5$, 392.1372; found, 392.1371. Actual charts are shown in Figures S19.

*1-(10H-phenoxazin-10-yl)-2-(4-nitorophenyl)ethanone (**6**)*.[30] From 2-(4-nitrophenyl)acetic acid (2.66 g, 14.7 mmol) and phenoxazine (2.2 g, 12.0 mmol), **6** was obtained as yellow solid (3.0 g, 7.0 mmol, 58% in isolated yield). Mp: 178 ~ 179 °C. ^{1}H NMR (600 MHz, $CDCl_3$, rt): δ 4.07 (s, 2H, -CH_2-), 7.13 (dd, J_{H-H} = 1.4, 8.2 Hz, 2H, *Phenoxazinyl*), 7.16 (ddd, 2H, J_{H-H} = 1.4, 8.2, 8.2 Hz, *Phenoxazinyl*), 7.24 (ddd, 2H, J_{H-H} = 1.4, 8.2, 8.2 Hz, *Phenoxazinyl*), 7.33 (d, 2H, J_{H-H} = 8.3 Hz, $C_6H_4NO_2$), 7.50 (dd, 2H, J_{H-H} = 1.4, 8.2 Hz, *Phenoxazinyl*), 8.13 (d, 2H, J_{H-H} = 8.3 Hz, $C_6H_4NO_2$). $^{13}C\{^1H\}$ NMR (151 MHz, $CDCl_3$, rt): δ 40.8, 117.2, 123.6, 123.7, 125.2, 127.6, 129.1, 130.3, 142.0, 147.1, 151.3, 169.0. IR (ATR, cm^{-1}) : 1669 (ν_{CO}). HRMS-EI(+) (m/z) : [M]+ calcd for $C_{20}H_{14}N_2O_4$, 346.0954; found, 346.0955. Actual charts are shown in Figures S20.

2-(4-Nitrophenyl)-N,N-diphenylpropionamide (7).[30] From 2-(4-nitrophenyl)propionic acid (6.2 g, 32.0 mmol) and diphenylamine (4.4 g, 26.0 mmol), **7** was obtained as yellow solid (7.9 g, 18.7 mmol, 72% in isolated yield). Mp: 119 ~ 120 °C. ^{1}H NMR (600 MHz, $CDCl_3$, –20 °C): δ 1.49 (d, J_{H-H} = 6.9 Hz, 3H, -CH_3), 3.96 (q, J_{H-H} = 6.9 Hz, 1H, -C*H*), 7.05 (br, 2H, *o-Ph*), 7.17 (d, J_{H-H} = 7.6 Hz, 2H, *o-Ph*), 7.19 (t, J_{H-H} = 7.6 Hz, 1H, *p-Ph*), 7.25 (d, J_{H-H} = 9.6

Hz, 2H, $C_6H_4NO_2$), 7.32 (dd, J_{H-H} = 7.6, 7.6 Hz, 2H, *m-Ph*), 7.35-7.40 (a mixture of broad signals, 3H, *m-Ph* and *p-Ph*), 8.12 (d, J_{H-H} = 9.6 Hz, 2H, $C_6H_4NO_2$). $^{13}C\{^1H\}$ NMR (151 MHz, $CDCl_3$, –20 °C): δ 20.5, 44.0, 123.9, 126.3, 126.6, 128.4, 128.6, 128.9, 129.1, 129.9, 141.9, 142.2, 146.7, 149.1, 172.9. IR (ATR, cm^{-1}) : 1662 (ν_{CO}). HRMS-EI(+) (m/z) : [M]+ calcd for $C_{21}H_{18}N_2O_3$, 346.1317; found, 346.1315. Actual charts are shown in Figures S21.

Preparation of 4-(2',1',3'-benzothiadiazol-4'-yl)-*N*,*N*-diphenylbenzeneacetamide (2f).[30] *Step 1: Synthesis of 4-(4',4',5',5'-tetramethyl-1',3',2'-dioxaborolan-2'-yl)-N,N-diphenylbenzeneacetamide (**2n**).* In a 100 ml of two-necked flask were placed **2d** (1.8 g, 5.0 mmol), $(Bpin)_2$ (1.5 g, 6.0 mmol), potassium acetate (1.3 g, 13.0 mmol) and 1,4-dioxane (15 mL). A mixture was stirred at ambient temperature for 20 min. After addition of $PdCl_2$(dppf) (183 mg, 0.25 mmol), the solution was heated at 105 °C under reflux in oil bath for 20 h. After cooling, brine (100 mL) was added, and the mixture was extracted with Et_2O (100 mL). Combined extracts were separated, and dried over Na_2SO_4. After filtration, the solution was concentrated *in vacuo*. The residue was purified by column chromatography (siliga-gel, eluted by hexane: EtOAc = 4: 1) to afford **2n** as white solid (3.4 g, 2.35 mmol, 47% isolated yield). Mp: 95.0 ~ 95.8 °C. ^1H NMR (600 MHz, $CDCl_3$, –20 °C): δ 1.34 (s, 12 H, CH_3), 3.68 (s, 2 H, CH_2), 7.12 (d, J_{H-H} = 8.2 Hz, 2H, C_6H_4Bpin), 7.14 (d, J_{H-H} = 7.6 Hz, 2H, *o-Ph*), 7.17

(t, J_{H-H} = 7.6 Hz, 1H, *p-Ph*), 7.21 (d, J_{H-H} = 7.6 Hz, 2H, *o-Ph*), 7.31 (dd, J_{H-H} = 7.6, 7.6 Hz, 2H, *m-Ph*), 7.35 (t, J_{H-H} = 7.6 Hz, 1H, *p-Ph*), 7.36 (dd, J_{H-H} = 7.6, 7.6 Hz, 2H, *m-Ph*), 7.70 (d, J_{H-H} = 8.2 Hz, 2H, C_6H_4Bpin). $^{13}C\{^1H\}$ NMR (151 MHz, $CDCl_3$, –20 °C): δ 24.9, 42.5, 83.9, 126.3, 126.4, 128.1, 128.5, 129.0, 129.0, 129.7, 134.9, 138.2, 142.4, 170.93. IR (ATR, cm^{-1}) : 1665 (ν_{CO}). HRMS-EI(+) (m/z) : [M]+ calcd for $C_{26}H_{28}BNO_3$, 413.2162; found, 413.2162. Actual charts are shown in Figures S17.

*Step 2: Synthesis of **2f**.* In a 500 ml of two-necked flask were placed **2n** (827 mg, 2.0 mmol), 4-bromobenzothiadiazole (430 mg, 2.0 mmol), toluene (120 mL) and EtOH (40 mL). The mixture was stirred at ambient temperature until the solid materials were completely dissolved. After addition of $Pd(PPh_3)_4$ (231 mg, 0.2 mmol) and K_2CO_3 (1.38 g, 10.0 mmol), the solution was heated at 80 °C in oil bath for 7 h. After cooling, H_2O (150 mL) was added, and the mixture was extracted with CH_2Cl_2 (150 mL). Extracts were separated, and dried over Na_2SO_4. After filtration, the solution was concentrated *in vacuo*. The residue was purified by column chromatography (silica gel, eluted by hexane: EtOAc = 4: 1) to afford **2f** as white solid (404 mg, 0.96 mmol, 48% isolated yield). Mp: 133.0 ~ 133.6 °C. ^1H NMR (600 MHz, $CDCl_3$, –20 °C): δ 3.74 (s, 2H, CH_2), 7.19 (t, J_{H-H} = 7.6 Hz, 1H, *p-Ph*), 7.26 (d,

J_{H-H} = 8.3 Hz, 2H, C_6H_4BTD), 7.26 (d, J_{H-H} = 8.3 Hz, 2H, *o-Ph*), 7.30 (d, J_{H-H} = 7.6 Hz, 2H, *o-Ph*), 7.33 (dd, J_{H-H} = 7.6, 7.6 Hz, 2H, *m-Ph*), 7.39 (t, J_{H-H} = 7.6 Hz, 1H, *p-Ph*), 7.44 (dd, J_{H-H} = 7.6, 7.6 Hz, 2H, *m-Ph*), 7.68-7.71 (a mixture of signals, 2H, *BTD*), 7.83 (d, J_{H-H} = 8.3 Hz, 2H, C_6H_4BTD), 7.99 (d, J_{H-H} = 4.8 Hz, 1H, *BTD*). $^{13}C\{^1H\}$ NMR (151 MHz, $CDCl_3$, –20 °C): δ 41.7, 120.5, 126.3, 126.4, 127.8, 128.2, 129.0, 129.0, 129.3, 129.5, 129.8, 129.9, 134.1, 135.3, 135.8, 142.4, 142.6, 153.4, 155.5, 171.0. IR (ATR, cm^{-1}) : 1656 (ν_{CO}). HRMS-EI(+) (m/z) : [M]+ calcd for $C_{26}H_{19}N_3OS$, 421.1249; found, 421.1248. Actual charts are shown in Figures S9.

Preparation of 2-(4-Acetylphenyl)-*N*,*N*-diphenylacetamide (2i).[30] In a 100 ml of two-necked flask were placed **2d** (2.2 g, 6.0 mmol), $Pd(OAc)_2$ (67 mg, 0.6 mmol), dppp (247 mg, 0.6 mmol), and [BMIM][OTf] (12 mL). After addition of 1-(vinyloxy)butane (3.8 mL, 30.0 mmol) and NEt_3 (1 mL, 7.2 mmol), the solution was heated at 115 °C in oil bath for 29 h. After cooling, 1M HCl aq. (42 ml) was added, and the mixture was extracted with CH_2Cl_2 (50 ml). The extracts were combined, washed with H_2O (50 mL), and dried over Na_2SO_4. After filtration, the solution was concentrated *in vacuo*. The residue was purified by column chromatography (silica-gel, eluted by hexane: EtOAc = 3: 1) to afford **2i** as white solid (1.1 g, 3.48 mmol, 58% in isolated yield). Mp: 112 ~ 113 °C. ^1H NMR (600 MHz, $CDCl_3$, –

20 °C): δ 2.61 (s, 3H, -CH_3), 3.72 (s, 2H, -CH_2-), 7.18 (d, J_{H-H} = 7.6 Hz, 2H, *o-Ph*), 7.19 (t, J_{H-H} = 7.6 Hz, 1H, *p-Ph*), 7.21 (d, J_{H-H} = 7.6 Hz, 2H, *o-Ph*), 7.22 (d, J_{H-H} = 8.3 Hz, 2H, $C_6H_4COCH_3$), 7.32 (dd, J_{H-H} = 7.6, 7.6 Hz, 2H, *m-Ph*), 7.38 (t, J_{H-H} = 7.6 Hz, 1H, *p-Ph*), 7.40 (dd, J_{H-H} = 7.6, 7.6 Hz, 2H, *m-Ph*), 7.87 (d, J_{H-H} = 8.3 Hz, 2H, $C_6H_4COCH_3$). $^{13}C\{^1H\}$ NMR (151 MHz, $CDCl_3$, –20 °C): δ 27.0, 42.1, 126.3, 126.4, 128.3, 128.5, 128.9, 129.0, 129.4, 129.9, 135.4, 140.6, 142.2, 142.2, 170.3, 198.4. IR (ATR, cm^{-1}) : 1667 (ν_{CONPh2} and ν_{COMe}, *overlapped*). HRMS-EI(+) (m/z) : [M]+ calcd for $C_{22}H_{19}NO_2$, 329.1416; found, 329.1417. Actual charts are shown in Figures S12.

Preparation of 2-(4-Formylphenyl)-*N*,*N*-diphenylacetamide (2k).[30] *Step 1: Synthesis of a mixture of 2-{4-(bromomethyl)phenyl}-N,N-diphenylacetamide (**2o**) and 2-{4-(chloromethyl)phenyl}-N,N-diphenylacetamide (**2p**).* In similar fashion to the general procedure described above, reaction of 2-{4-(bromomethyl)phenyl}acetic acid (2.3 g, 10.0 mmol) with $SOCl_2$ was followed by treatment of the resulting acyl chloride with diphenylamine (1.4 g, 8.0 mmol). During the reaction with $SOCl_2$, a part of bromomethyl group of 2-{4-(bromomethyl)phenyl}acetic acid was converted to the chloromethyl moiety. The products were a 75 : 25 mixture of **2o** and **2p** determined by ^1H NMR (pale yellow solid, 7.3 g, 24 mmol for 75 : 25 mixture of **2o** and **2p**). Mp : 124.6 ~ 126.6 °C. ^1H NMR (600

MHz, $CDCl_3$, -20°C) δ : 3.66 (s, 2H, -CH_2CO- of **2o**), 3.66 (s, 2H, -CH_2CO- of **2p**), 4.49 (s, 2H, -CH_2Br of **2o**), 4.58 (s, 2H, -CH_2Cl of **2p**) 7.10 (d, $J_{H\text{-}H}$ = 8.3 Hz, 2H, $C_6H_4CH_2Br$ of **2o**), 7.12 (d, $J_{H\text{-}H}$ = 8.3 Hz, 2H, $C_6H_4CH_2Cl$ of **2p**), 7.18 (t, $J_{H\text{-}H}$ = 8.3 Hz, 1H, *p-Ph*), 7.18(d, $J_{H\text{-}H}$ = 7.6 Hz, 2H, *o-Ph*), 7.24 (d, $J_{H\text{-}H}$ = 7.6 Hz, 2H, *o-Ph*), 7.29 (d, $J_{H\text{-}H}$ = 7.6 Hz, 2H, C_6H_4), 7.32 (dd, $J_{H\text{-}H}$ = 7.6, 7.6 Hz, 2H, *m-Ph*), 7.37 (t, $J_{H\text{-}H}$ = 7.6 Hz, 1H, *p-Ph*), 7.40 (dd, $J_{H\text{-}H}$ = 7.6, 7.6 Hz, 2H, *m-Ph*). $^{13}C\{^1H\}$ NMR (151 MHz, $CDCl_3$, -20°C) δ : 33.8, 41.8 (**2o**), 46.3 (**2p**), 126.3, 128.2, 128.8 (**2p**), 128.9 (**2o**), 129.0, 129.2, 129.5 (**2p**), 129.5 (**2o**), 129.8, 135.3 (**2p**), 135.4 (**2o**), 135.8 (**2p**), 136.2 (**2o**), 142.3, 142.4, 170.9. IR (ATR, cm^{-1}) : 1681 (ν_{CO}). HRMS-EI(+) (m/z) : [M]+ calcd for $C_{21}H_{18}NOBr$, 379.0572; found, 379.0574. Actual charts are shown in Figures S18.

*Step 2. Synthesis of 2-(4-formylphenyl)-N,N-diphenylacetamide (**2k**).* In a 30 ml of two-necked flask were placed a 75: 25 mixture of **2o** and **2p** (1.14 g, 3.0 mmol for 75 : 25 mixture of **2o** and **2p**), hexamethylenetetramine (1.26 g, 9.0 mmol), EtOH (6 mL) and H_2O (6 mL). The solution was heated at 100 °C in oil bath for 4 h. Addition of conc. HCl (1.5 mL) was followed by additional heating at 100 °C in oil bath for 30 minutes. After cooling, the organic products were extracted with CH_2Cl_2. The extracts were combined, washed with H_2O, and dried over $MgSO_4$. After filtration, the solution was concentrated *in vacuo*. The residue was

purified by column chromatography (silica gel, eluted by hexane: EtOAc = 3: 7) to afford **2k** (652 mg, 2.07 mmol, 69% in isolated yield). Mp : 90.4 ~ 91.7 °C. ^{1}H NMR (600 MHz, $CDCl_3$, –20 °C): δ 3.74 (s, 2H, -CH_2-), 7.19 (t, J_{H-H} = 7.6 Hz, 1H, *p-Ph*), 7.20 (d, J_{H-H} = 7.6 Hz, 2H, *o-Ph*), 7.23 (d, J_{H-H} = 7.6 Hz, 2H, *o-Ph*), 7.29 (d, J_{H-H} = 8.3 Hz, 2H, C_6H_4CHO), 7.32 (dd, J_{H-H} = 7.6, 7.6 Hz, 2H, *m-Ph*), 7.38 (t, J_{H-H} = 7.6 Hz, 1H, *p-Ph*), 7.42 (dd, J_{H-H} = 7.6, 7.6 Hz, 2H, *m-Ph*), 7.79 (d, J_{H-H} = 8.3 Hz, 2H, C_6H_4CHO), 9.98 (s, 1H, C*H*O). ^{13}C{^{1}H} NMR (151 MHz, $CDCl_3$, –20 °C): δ 42.3, 126.3, 126.5, 128.4, 128.9, 129.0, 129.9, 129.9, 130.0, 134.8, 142.1, 142.2, 142.2, 170.1, 192.5. IR (ATR, cm^{-1}) : 1657 (ν_{CONPh2}), 1691 (ν_{CHO}). HRMS-EI(+) (m/z) : [M]+ calcd for $C_{21}H_{17}NO_2$, 315.1259; found, 315.1259. Actual charts are shown in Figures S13.

Preparation of 4-(4'-Nitrophenyl)-*N*,*N*-diphenylbenzeneacetamide (8).[30] In a 500 ml of two-necked flask were added **2n** (827 mg, 2.0 mmol), 4-bromonitrobenzene (404 mg, 2.0 mmol), toluene (120 mL) and EtOH (40 mL). A mixture was stirred at ambient temperature until solids were completely dissolved. After addition of $Pd(PPh_3)_4$ (231 mg, 0.2 mmol) and K_2CO_3 (1.38 g, 10.0 mmol), the solution was heated at 80 °C in oil bath for 12 h. After cooling, H_2O (100 mL) was added, and the mixture was extracted with CH_2Cl_2 (100 mL). The extracts were combined, and dried over Na_2SO_4. After filtration, the solution was

concentrated *in vacuo*. The residue was purified by chromatography (siliga gel, eluted by hexane: EtOAc = 4: 1) to afford amide **8** (687 mg, 1.68 mmol, 84% isolated yield). Mp : 131.4 ~ 132.5 °C. ^{1}H NMR (600 MHz, $CDCl_3$, –20 °C): δ 3.71 (s, 2H, -CH_2-), 7.19 (t, J_{H-H} = 7.6 Hz, 1H, *p-Ph*), 7.23-7.27 (a mixture of signals, 6H, *o-Ph* and $(C_6H_4)_2NO_2$), 7.32 (dd, J_{H-H} = 7.6, 7.6 Hz, 2H, *m-Ph*), 7.41 (t, J_{H-H} = 7.6 Hz, 1H, *p-Ph*), 7.43 (dd, J_{H-H} = 7.6, 7.6 Hz, 2H, *m-Ph*), 7.54 (d, J_{H-H} = 8.3 Hz, 2H, $(C_6H_4)_2NO_2$), 7.73 (d, J_{H-H} = 8.3 Hz, 2H, $(C_6H_4)_2NO_2$), 8.29 (d, J_{H-H} = 8.3 Hz, 2H, $(C_6H_4)_2NO_2$). ^{13}C{^{1}H} NMR (151 MHz, $CDCl_3$, –20 °C): δ 41.8, 124.3, 126.4, 126.4, 127.5, 127.7, 128.3, 129.0, 129.0, 129.9, 130.1, 136.0, 137.1, 142.3, 142.5, 146.7, 147.3, 170.9. IR (ATR, cm^{-1}) : 1664 (ν_{CO}). HRMS-EI(+) (m/z) : [M]+ calcd for $C_{26}H_{20}N_2O_3$, 408.1474; found, 408.1473. Actual charts are shown in Figure S22.

Preparation of 4,7-Bis(*N*,*N*-diphenyl-4'-carbamoylmethylphenyl-)-2,1,3-benzothidiazole (13).[30] In a 500 ml of two-necked flask were placed **2n** (2.07 g, 5.0 mmol), 2,7-dibromobenzothiadiazole (735 mg, 2.5 mmol), toluene (150 mL) and EtOH (50 mL). A mixture was stirred at ambient temperature until solids were completely dissolved. Addition of $Pd(PPh_3)_4$ (578 mg, 0.5 mmol) and K_2CO_3 (3.45 g, 25.0 mmol) was followed by heating the solution at 80 °C in oil bath for 14 h. After cooling, H_2O (100 mL) was added, and the mixture was extracted with CH_2Cl_2 (100 mL). Extracts were combined, and dried over

Na_2SO_4. After filtration, the solution was concentrated *in vacuo*. The residue was purified by column chromatography (siliga-gel eluted by hexane: EtOAc = 2: 1) to afford amide **13** (775 mg, 1.10 mmol, 44% isolated yield). Mp: 153.9 ~ 154.8 °C. ^{1}H NMR (600 MHz, $CDCl_3$, –20 °C): δ 3.75 (s, 4H, -CH_2-), 7.19 (t, J_{H-H} = 7.6 Hz, 2H, *p-Ph*), 7.27 (d, J_{H-H} = 7.6 Hz, 4H, *o-Ph*), 7.28 (d, J_{H-H} = 8.3 Hz, 4H, C_6H_4BTD), 7.32 (d, J_{H-H} = 7.6 Hz, 4H, *o-Ph*), 7.33 (dd, J_{H-H} = 7.6, 7.6 Hz, 4H, *m-Ph*), 7.39 (t, J_{H-H} = 7.6 Hz, 2H, *p-Ph*), 7.44 (dd, J_{H-H} = 7.6, 7.6 Hz, 4H, *m-Ph*), 7.78 (s, 2H, -BTD-), 7.87 (d, J_{H-H} = 8.3 Hz, 4H, C_6H_4BTD). ^{13}C{^{1}H} NMR (151 MHz, $CDCl_3$, –20 °C): δ 41.7, 126.4, 126.4, 128.2, 128.3, 129.0, 129.0, 129.3, 129.5, 129.9, 132.8, 135.3, 135.9, 142.4, 142.6, 154.0, 171.1. IR (ATR, cm^{-1}) : 1661 (ν_{CO}). HRMS-EI(+) (m/z) : [M]+ calcd for $C_{46}H_{34}N_4O_2S$, 706.2402; found, 706.2403. Actual charts are shown in Figures S39.

General procedure for the preparation of D-π-A enamines 4, 9-12. In a 20 mL two-necked recovery flask was placed the amide (0.50 ~ 2.00 mmol). Addition of the iridium catalyst **1X** or **1Y** was followed by the addition of toluene (5.0 ~ 20 mL total), anisole (1 equiv. toward the amide, as an internal standard) and TMDS (2 equiv. to the amide). The mixture was stirred at the temperature for the time described in Tables 1-4 and Scheme 1. The conversion of amides and yields of enamines or silylhemiaminals were determined by

^{1}H NMR spectroscopy based on the internal standard. After the reaction, the resulting silane residue including unreacted TMDS and the solvent were removed *in vacuo*. The obtained viscous solid was again dissolved in toluene (15 mL) and heated at 60 °C in oil bath for 1 h to convert the silylhemiaminal to the corresponding enamine. The solution was concentrated under reduced pressure. The solid obtained was rinsed with cold pentane (–78 °C, 10 mL × 3) and dried *in vacuo*. Chromatographic purification (silica gel, eluted by hexane : EtOAc : NEt_3 = 100 : 10 : 1) gave the desired enamines.

*N-{2-(4-fluorophenyl)ethenyl}-N-phenylbenzenamine (**4b**)*.[30] The reaction of **2b** (305 mg, 1.00 mmol) with TMDS (268.8 mg, 2.00 mmol) was performed in the presence of **1X** (0.05 mol%) in toluene (10 mL) at 25 °C in oil bath for 2 h. The product **4b** was obtained as a white solid (262 mg, 0.91 mmol, 91%). Mp: 75.4 ~ 76.4 °C. ^{1}H NMR (400 MHz, $CDCl_3$, r.t.): δ 5.58 (d, $J_{H\text{-}H}$ = 14.1 Hz, 1H, CH=C*H*), 6.93 (dd, $J_{H\text{-}H}$ = 8.7 Hz, $J_{H\text{-}F}$ = 8.7 Hz, 2H, C_6H_4F), 7.11 (d, $J_{H\text{-}H}$ = 8.7 Hz, 4H, *o-Ph*), 7.14 (t, $J_{H\text{-}H}$ = 7.8 Hz, 2H, *p-Ph*), 7.15 (dd, $J_{H\text{-}H}$ = 8.7 Hz, $J_{H\text{-}F}$ = 5.3 Hz, 2H, C_6H_4F), 7.29 (d, $J_{H\text{-}H}$ = 14.1 Hz, 1H, C*H*=CH), 7.36 (dd, $J_{H\text{-}H}$ = 8.7, 7.8 Hz, 4H, *m-Ph*). ^{13}C{^{1}H} NMR (100 MHz, $CDCl_3$, r.t.): δ 108.1, 115.5 (d, $J_{C\text{-}F}$ = 20.2 Hz), 123.8, 124.1, 126.09, 125.7 (d, $J_{C\text{-}F}$ = 7.7 Hz), 133.5, 134.4 (d, $J_{C\text{-}F}$ = 2.9 Hz), 145.4, 160.9 (d, $J_{C\text{-}F}$ = 243.7 Hz). ^{19}F{^{1}H} NMR (376 MHz, $CDCl_3$, r.t.): δ –118.13. IR (ATR, cm^{-1}): 1637,

1586 ($\nu_{C=CN}$). HRMS-EI(+) (m/z): $[M]^+$ calcd for $C_{20}H_{16}NF$ 289.1267; found 289.1264. Actual charts are shown in Figures S23.

*N-{2-(4-chlorophenyl)ethenyl}-N-phenylbenzenamine (**4c**).*[30] The reaction of **2c** (322 mg, 1.00 mmol) with TMDS (268.8 mg, 2.00 mmol) was performed in the presence of **1X** (0.05 mol%) in toluene (10 mL) at 25 °C in oil bath for 4 h. The product **4c** was obtained as a white solid (217 mg, 0.71 mmol, 71%). Mp: 109.3 ~ 109.8 °C. ^{1}H NMR of **4c** (400 MHz, $CDCl_3$, r.t.): δ 5.53 (d, J_{H-H} = 14.2 Hz, 1H, CH=C*H*), 7.10 (d, J_{H-H} = 8.7 Hz, 4H, *o-Ph*), 7.12 (d, J_{H-H} = 8.7 Hz, 2H, C_6H_4Cl), 7.15 (t, J_{H-H} = 7.8 Hz, 2H, *p-Ph*), 7.19 (d, J_{H-H} = 8.7 Hz, 2H, C_6H_4Cl), 7.36 (dd, J_{H-H} = 7.8, 8.7 Hz, 4H, *m-Ph*), 7.36 (d, J_{H-H} = 14.2 Hz, 1H, C*H*=CH). $^{13}C\{^1H\}$ NMR of **4c** (100 MHz, $CDCl_3$, r.t.): δ 107.6, 123.9, 124.3, 125.7, 128.8, 129.7, 130.2, 134.2, 136.9, 145.3. IR (ATR, cm^{-1}): 1633, 1585 ($\nu_{C=CN}$). HRMS-EI(+) (m/z): $[M]^+$ calcd for $C_{20}H_{16}NCl$ 305.0971; found 305.0969. Actual charts are shown in Figures S24.

*N-{2-(4-bromophenyl)ethenyl}-N-phenylbenzenamine (**4d**).*[30] The reaction of **2d** (183 mg, 0.50 mmol) with TMDS (134.4 mg, 1.00 mmol) was performed in the presence of **1Y** (0.03 mol%) in toluene (5 ml) at 30 °C in oil bath for 2 h. The product **4d** was obtained as a white solid (144 mg, 0.41 mmol, 82%). Mp: 107.5 ~ 108.0 °C. ^{1}H NMR (400 MHz, $CDCl_3$, r.t.): δ 5.51 (d, J_{H-H} = 14.2 Hz, 1H, CH=C*H*), 7.06 (d, J_{H-H} = 8.3 Hz, 2H, C_6H_4Br), 7.10 (d, J_{H-H} =

8.7 Hz, 4H, *o-Ph*), 7.14 (t, J_{H-H} = 7.8 Hz, 2H, *p-Ph*), 7.33 (d, J_{H-H} = 8.3 Hz, 2H, C_6H_4Br), 7.36 (dd, J_{H-H} = 7.8, 8.7 Hz, 4H, *m-Ph*), 7.38 (d, J_{H-H} = 14.2 Hz, 1H, C*H*=CH). $^{13}C\{^1H\}$ NMR (100 MHz, $CDCl_3$, r.t.): δ 107.6 118.1, 123.9, 124.3, 126.0, 129.7, 131.7, 134.2, 137.4, 145.3. IR (ATR, cm^{-1}): 1632, 1588, 1579 ($\nu_{C=CN}$). HRMS-EI(+) (m/z): $[M]^+$ calcd for $C_{20}H_{16}NBr$ 349.0466; found 349.0467. Actual charts are shown in Figures S25.

*N-{2-(4-iodophenyl)ethenyl}-N-phenylbenzenamine (**4e**).* The reaction of **2e** (207 mg, 0.50 mmol) with TMDS (134.4 mg, 1.00 mmol) was performed in the presence of **1Y** (0.3 mol%) in toluene (5 mL) at 30 °C in oil bath for 6 h. The product **4e** was obtained as a white solid (143 mg, 0.36 mmol, 72%). Mp: 106.0 ~ 106.3 °C. ^1H NMR (400 MHz, $CDCl_3$, r.t.): δ 5.49 (d, J_{H-H} = 14.2 Hz, 1H, CH=C*H*), 6.94 (d, J_{H-H} = 8.7 Hz, 2H, C_6H_4I), 7.10 (d, J_{H-H} = 8.2 Hz, 4H, *o-Ph*), 7.14 (t, J_{H-H} = 7.7 Hz, 2H, *p-Ph*), 7.35 (dd, J_{H-H} = 8.3, 7.7 Hz, 4H, *m-Ph*), 7.39 (d, J_{H-H} = 14.2 Hz, 1H, C*H*=CH), 7.52 (d, J_{H-H} = 8.7 Hz, 2H, C_6H_4I). $^{13}C\{^1H\}$ NMR (100 MHz, $CDCl_3$, r.t.): δ 88.8, 107.6, 123.9, 124.4, 126.4, 129.7, 134.3, 137.6, 138.0, 145.2. IR (ATR, cm^{-1}): 1632, 1586, 1577 ($\nu_{C=CN}$). HRMS-EI(+) (m/z): $[M]^+$ calcd for $C_{20}H_{16}NI$ 397.0328; found 397.0329. Actual charts are shown in Figures S26.

*N-[2-{4-(2',1',3'-benzothiadiazol-4'-yl)phenyl}ethenyl]-N-phenylbenzenamine (**4f**).*[30] The reaction of **2f** (211 mg, 0.50 mmol) with TMDS (134.4 mg, 1.00 mmol) was performed in

the presence of **1Y** (0.5 mol%) in toluene (5 mL) at 30 °C in oil bath for 2 h. The product **4f** was obtained as a red solid (89 mg, 0.21 mmol, 42%). Mp: 134.3 ~ 135.0 °C. ^{1}H NMR (400 MHz, $CDCl_3$, r.t.): δ 5.69 (d, J_{H-H} = 14.3 Hz, 1H, CH=C*H*), 7.14 (d, J_{H-H} = 8.2 Hz, 2H, *o-Ph*), 7.16 (t, J_{H-H} = 8.2 Hz, 2H, *p-Ph*), 7.36 (d, J_{H-H} = 8.2 Hz, 2H, C_6H_4BTD), 7.38 (dd, J_{H-H} = 8.3, 7.7 Hz, 4H, *m-Ph*), 7.50 (d, J_{H-H} = 14.3 Hz, 1H, C*H*=CH), 7.64-7.69 (a mixture of signals, 1H+1H, BTD), 7.85 (d, J_{H-H} = 8.2 Hz, 2H, C_6H_4BTD), 7.96 (d, J_{H-H} = 8.2 Hz, 1H, BTD). ^{13}C{^{1}H} NMR (100 MHz, $CDCl_3$, r.t.): δ 102.3, 111.5, 112.3, 114.6, 114.9, 115.2, 117.0, 119.1, 119.2, 119.3, 122.5, 122.9, 123.1, 126.5, 131.7, 140.1. IR (ATR, cm^{-1}): 1632, 1587 ($\nu_{C=CN}$). HRMS-EI(+) (m/z): $[M]^+$ calcd for $C_{26}H_{19}N_3S$ 405.1300; found 405.1300. Actual charts are shown in Figures S27.

*N-{2-(4-cyanophenyl)ethenyl}-N-phenylbenzenamine (**4g**).*[30] The reaction of **2g** (166 mg, 0.50 mmol) with TMDS (134.4 mg, 1.00 mmol) was performed in the presence of **1Y** (0.5 mol%) in toluene (5 mL) at 30 °C in oil bath for 1 h. The product **4g** was obtained as a yellow solid (86 mg, 0.29 mmol, 58%). Mp.: 113 ~ 114 °C. ^{1}H NMR (400 MHz, $CDCl_3$, r.t.): δ 5.52 (d, J_{H-H} = 14.2 Hz, 1H, CH=C*H*), 7.11 (d, J_{H-H} = 8.7 Hz, 4H, *o-Ph*), 7.19 (t, J_{H-H} = 7.8 Hz, 2H, *p-Ph*), 7.22 (d, J_{H-H} = 8.7 Hz, 2H, C_6H_4CN), 7.38 (dd, J_{H-H} = 7.8, 8.7 Hz, 4H, *m-Ph*), 7.47 (d, J_{H-H} = 8.7 Hz, 2H, C_6H_4CN), 7.55 (d, J_{H-H} = 14.2 Hz, 1H, C*H*=CH). ^{13}C{^{1}H} NMR

(100 MHz, $CDCl_3$, r.t.): δ 106.4, 107.0, 119.9, 124.1, 124.5, 125.0, 129.8, 132.5, 136.7, 143.6, 144.9. IR (ATR, cm^{-1}): 2215 ($\nu_{C\equiv N}$), 1671, 1632, 1583 ($\nu_{C=CN}$). HRMS-EI(+) (m/z): $[M]^+$ calcd for $C_{21}H_{16}N_2$ 296.1313; found 296.1313. Actual charts are shown in Figures S28.

*N-[2-{4-(methoxycarbonyl)phenyl}ethenyl]-N-phenylbenzenamine (**4h**).* The reaction of **2h** (173 mg, 0.50 mmol) with TMDS (134.4 mg, 1.00 mmol) was performed in the presence of **1X** (0.1 mol%) in CH_2Cl_2 (1 mL) at 30 °C in oil bath for 19 h. The product **4h** was obtained as a yellow solid (102 mg, 0.31 mmol, 61%). Mp: 107.5 ~ 108.0 °C. ^{1}H NMR (400 MHz, $CDCl_3$, r.t.): δ 3.88 (s, 3H, -OC*H₃*), 5.57 (d, J_{H-H} = 13.5 Hz, 1H, CH=C*H*), 7.12 (d, J_{H-H} = 8.3 Hz, 4H, *o-Ph*), 7.17 (t, J_{H-H} = 8.3 Hz, 2H, *p-Ph*), 7.22 (d, J_{H-H} = 8.7 Hz, 2H, $C_6H_4CO_2Me$), 7.37 (dd, J_{H-H} = 8.3, ,8.3 Hz, 4H, *m-Ph*), 7.55 (d, J_{H-H} = 13.5 Hz, 1H, C*H*=CH), 7.88 (d, 2H, J_{H-H} = 8.7 Hz, $C_6H_4CO_2Me$). $^{13}C\{^1H\}$ NMR (100 MHz, $CDCl_3$, r.t.): δ 52.0, 107.4, 124.0, 124.0, 124.7, 126.1, 129.7, 130.2, 135.8, 143.5, 145.0, 167.3. IR (ATR, cm^{-1}): 1669 ($\nu_{C=O}$), 1630, 1583 ($\nu_{C=CN}$). HRMS-EI(+) (m/z): $[M]^+$ calcd for $C_{22}H_{19}NO_2$ 329.1416; found 329.1416. Actual charts are shown in Figures S29.

*N-{2-(4-acetylphenyl)ethenyl}-N-phenylbenzenamine (**4i**).*[30] The reaction of **2i** (165 mg, 0.50 mmol) with TMDS (134.4 mg, 1.00 mmol) was performed in the presence of **1X** (0.25 mol%) in toluene (5 mL) at 30 °C in oil bath for 2 h. The product **4i** was obtained as a yellow

solid (106 mg, 0.34 mmol, 68%). Mp: 115 ~ 116 °C. ^{1}H NMR (400 MHz, $CDCl_3$, r.t.): δ 2.55 (s, 3H, -C*H*$_3$), 5.57 (d, J_{H-H} = 13.7 Hz, 1H, CH=C*H*), 7.12 (d, J_{H-H} = 8.3 Hz, 4H, *o-Ph*), 7.18 (t, J_{H-H} = 8.3 Hz, 2H, *p-Ph*), 7.24 (d, J_{H-H} = 8.7 Hz, 2H, C_6H_4COMe), 7.38 (dd, J_{H-H} = 8.3, 8.3 Hz, 4H, *m-Ph*), 7.57 (d, J_{H-H} = 13.7 Hz, 1H, C*H*=CH), 7.82 (d, J_{H-H} = 8.7 Hz, 2H, C_6H_4COMe). ^{13}C{^{1}H} NMR of **4i** (100 MHz, $CDCl_3$, r.t.): δ 26.5, 107.2, 118.0, 124.1, 124.8, 129.2, 129.8, 133.5, 136.1, 143.9, 145.0, 197.4. IR (ATR, cm^{-1}): 1662 ($\nu_{C=O}$), 1631, 1579 ($\nu_{C=CN}$). HRMS-EI(+) (m/z): [M]$^{+}$ calcd for $C_{22}H_{19}NO$ 313.1467; found 313.1466. Actual charts are shown in Figures S30.

*N-{2-(4-formylphenyl)ethenyl}-N-phenylbenzenamine (**4k**).*[30] The reaction of **2k** (152 mg, 0.50 mmol) with TMDS (134.4 mg, 1.00 mmol) was performed in the presence of **1X** (0.1 mol%) in toluene (5 mL) at 25 °C in oil bath for 2 h. The product **4k** was obtained as a yellow solid (67 mg, 0.22 mmol, 44%). Mp: 102.4 ~ 103.0 °C. ^{1}H NMR (400 MHz, $CDCl_3$, r.t.): δ 5.58 (d, J_{H-H} = 14.2 Hz, 1H, CH=C*H*), 7.13 (d, J_{H-H} = 8.3 Hz, 4H, *o-Ph*), 7.19 (t, J_{H-H} = 8.3 Hz, 2H, *p-Ph*), 7.30 (d, J_{H-H} = 8.7 Hz, 2H, C_6H_4CHO), 7.38 (dd, J_{H-H} = 8.3, 8.3 Hz, 4H, *m-Ph*), 7.62 (d, J_{H-H} = 14.2 Hz, 1H, C*H*=CH), 7.72 (d, J_{H-H} = 8.7 Hz, 2H, C_6H_4CHO), 9.87 (s, 1H, -C*H*O). ^{13}C{^{1}H} NMR (100 MHz, $CDCl_3$, r.t.): δ 106.9, 124.1, 124.4, 125.0, 129.8, 130.6, 133.0, 136.7, 144.8, 145.5, 191.5. IR (ATR, cm^{-1}): 1685 ($\nu_{C=O}$), 1632, 1577, 1558 ($\nu_{C=CN}$).

HRMS-EI(+) (m/z): $[M]^+$ calcd for $C_{21}H_{17}NO$ 299.1310; found 299.1310. Actual charts are shown in Figures S31.

*N-{2-(4-nitrophenyl)ethenyl}-N-phenylbenzenamine (**4m**).*[30] The reaction of **2m** (166 mg, 0.50 mmol) with TMDS (134.4 mg, 1.00 mmol) was performed in the presence of **1Y** (0.5 mol%) in toluene (5 mL) at 30 °C in oil bath for 6 h. The product **4m** was obtained as a red solid (97 mg, 0.31 mmol, 61%). Mp: 149.6 ~ 150.9 °C. ^{1}H NMR (400 MHz, $CDCl_3$, r.t.): δ 5.56 (d, J_{H-H} = 13.5 Hz, 1 H, CH=C*H*), 7.13 (d, J_{H-H} = 8.3 Hz, 4 H, *o-Ph*), 7.21 (t, J_{H-H} = 8.3 Hz, 2H, *p-Ph*), 7.24 (d, J_{H-H} = 8.7 Hz, 2H, $C_6H_4NO_2$), 7.40 (dd, J_{H-H} = 8.3, 8.3 Hz, 4H, *m-Ph*), 7.64 (d, J_{H-H} = 13.5 Hz, 1H, C*H*=CH), 8.07 (d, J_{H-H} = 8.7 Hz, 1H, $C_6H_4NO_2$). ^{13}C{^{1}H} NMR (100 MHz, $CDCl_3$, r.t.): δ 105.9, 124.0, 124.2, 124.5, 125.3, 129.5, 129.9, 137.6, 144.4, 144.7. IR (ATR, cm^{-1}): 1631, 1576 ($\nu_{C=CN}$). HRMS-EI(+) (m/z): $[M]^+$ calcd for $C_{20}H_{16}N_2O_2$ 316.1212; found 316.1211. Actual charts are shown in Figures S32.

*N-{2-(3-nitrophenyl)ethenyl}-N-phenylbenzenamine (**4m'**).*[30] The reaction of **2m'** (166 mg, 0.50 mmol) with TMDS (134.4 mg, 1.00 mmol) was performed in the presence of **1Y** (0.5 mol%) in toluene (5 mL) at 30 °C in oil bath for 6 h. The product **4m'** was obtained as an orange solid (116 mg, 0.37 mmol, 73%). Mp: 86.0 ~ 86.1 °C. ^{1}H NMR (400 MHz, $CDCl_3$, r.t.): δ 5.56 (d, J_{H-H} = 13.7 Hz, 1H, CH=C*H*), 7.12 (d, J_{H-H} = 8.3 Hz, 4H, *o-Ph*), 7.19 (t, J_{H-H}

= 7.3 Hz, 2H, *p-Ph*), 7.35 (dd, J_{H-H} = 8.2, 8.2 Hz, 1H, $C_6H_4NO_2$), 7.38 (dd, J_{H-H} = 7.3, 8.3 Hz, 4H, *m-Ph*), 7.45 (d, J_{H-H} = 8.2 Hz, 1H, $C_6H_4NO_2$), 7.54 (d, J_{H-H} = 13.7 Hz, 1H, C*H*=CH), 7.86 (d, J_{H-H} = 8.2 Hz, 1H, $C_6H_4NO_2$), 8.02 (s, 1H, $C_6H_4NO_2$). $^{13}C\{^1H\}$ NMR (100 MHz, $CDCl_3$, r.t.): δ 105.8, 118.7, 119.2, 124.0, 124.8, 129.4, 129.8, 130.1, 135.9, 140.6, 144.9, 148.9. IR (ATR, cm^{-1}): 1635, 1586 ($\nu_{C=CN}$). HRMS-EI(+) (m/z): $[M]^+$ calcd for $C_{20}H_{16}N_2O_2$ 316.1212; found 316.1212. Actual charts are shown in Figures S33.

*N-{2-(2-nitrophenyl)ethenyl}-N-phenylbenzenamine (**4m”**).*[30] The reaction of **2m”** (166 mg, 0.50 mmol) with TMDS (134.4 mg, 1.00 mmol) was performed in the presence of **1Y** (0.5 mol%) in toluene (5 mL) at 30 °C in oil bath for 6 h. The product **4m”** was obtained as a red paste (119 mg, 0.38 mmol, 75%). Mp: 49.1 ~ 49.2 °C. ^1H NMR (400 MHz, $CDCl_3$, r.t.): δ 6.16 (d, J_{H-H} = 13.7 Hz, 1H, CH=C*H*), 7.13 (d, J_{H-H} = 8.3 Hz, 4H, *o-Ph*), 7.14 (1H, $C_6H_4NO_2$, overlapped with *o-Ph* and *p-Ph* and determined by ^1H-^1H COSY), 7.18 (t, J_{H-H} = 7.7 Hz, 2H, *p-Ph*), 7.37 (dd, J_{H-H} = 7.7, 8.7 Hz, 4H, *m-Ph*), 7.45 (dd, J_{H-H} = 7.7, 7.7 Hz, 1H, $C_6H_4NO_2$), 7.57 (d, J_{H-H} = 13.7 Hz, 1H, C*H*=CH), 7.60 (d, J_{H-H} = 7.7 Hz, 1H, $C_6H_4NO_2$), 7.84 (d, J_{H-H} = 7.7 Hz, 1H, $C_6H_4NO_2$). $^{13}C\{^1H\}$ NMR (100 MHz, $CDCl_3$, r.t.): δ 102.9, 124.0, 124.9, 125.0, 125.3, 126.2, 129.8, 132.9, 134.4, 137.9, 144.9, 146.5. IR (ATR, cm^{-1}): 1629,

1587 ($\nu_{C=CN}$). HRMS-EI(+) (m/z): $[M]^+$ calcd for $C_{20}H_{16}N_2O_2$ 316.1212; found 316.1211. Actual charts are shown in Figures S34.

*N-{2-(4-nitrophenyl)ethenyl}-N,N-di(4'-methoxyphenyl)amine (**9**).*[30] The reaction of **9** (196 mg, 0.50 mmol) with TMDS (134.4 mg, 1.00 mmol) was performed in the presence of **1Y** (0.5 mol%) in toluene (5 mL) at 30 °C in oil bath for 6 h. The product **9** was obtained as a dark red solid (151 mg, 0.40 mmol, 79%). Mp: 115.5 ~ 115.6 °C. ^{1}H NMR (400 MHz, $CDCl_3$, r.t.): δ 3.83 (s, 6H, -OC*H*$_3$), 5.47 (d, J_{H-H} = 13.7 Hz, 1H, CH=C*H*), 6.91 (d, J_{H-H} = 8.3 Hz, 4H, $C_6H_4OCH_3$), 7.05 (d, J_{H-H} = 8.3 Hz, 4H, $C_6H_4OCH_3$), 7.20 (d, J_{H-H} = 8.7 Hz, 2H, $C_6H_4NO_2$), 7.56 (d, J_{H-H} = 13.7 Hz, 1H, C*H*=CH), 8.05 (d, J_{H-H} = 8.7 Hz, 2H, $C_6H_4NO_2$). ^{13}C{^{1}H} NMR (100 MHz, $CDCl_3$, r.t.): δ 55.7, 104.0, 115.0, 123.6, 124.6, 125.4, 138.2, 138.7, 143.9, 146.7, 157.3. IR (ATR, cm^{-1}): 1626, 1577 ($\nu_{C=CN}$). HRMS-EI(+) (m/z): $[M]^+$ calcd for $C_{22}H_{20}N_2O_4$ 376.1423; found 376.1424. Actual charts are shown in Figures S35.

*10-{2-(4-nitrophenyl)ethenyl}-10H-phenoxazine (**10**).*[30] The reaction of **6** (173 mg, 0.50 mmol) with TMDS (134.4 mg, 1.00 mmol) was performed in the presence of **1Y** (0.5 mol%) in toluene (5 mL) at 30 °C in oil bath for 6 h. The product **10** was obtained as a red solid (66 mg, 0.20 mmol, 40%). Mp: 178 ~ 179 °C. ^{1}H NMR (400 MHz, $CDCl_3$, r.t.): δ 6.55 (d, J_{H-H} = 14.6 Hz, 1H, CH=C*H*), 7.01 (dd, J_{H-H} = 7.7, 1.4 Hz, 2H, -N(C_6H_4)$_2$O), 7.06 (ddd, J_{H-H} =

7.7, 7.7, 1.4 Hz, 2H, -N(C_6H_4)$_2$O), 7.10 (ddd, J_{H-H} = 7.7, 7.7, 1.4 Hz, 2H, -N(C_6H_4)$_2$O), 7.29 (dd, J_{H-H} = 7.7, 1.4 Hz, 2H, -N(C_6H_4)$_2$O), 7.35 (d, J_{H-H} = 8.7 Hz, 2H, $C_6H_4NO_2$), 7.39 (d, J_{H-H} = 14.6 Hz, 1H, C*H*=CH), 8.13 (d, J_{H-H} = 8.7 Hz, 2H, $C_6H_4NO_2$). $^{13}C\{^1H\}$ NMR **10** (100 MHz, $CDCl_3$, r.t.): δ 105.1, 117.3, 119.1, 124.0, 124.5, 124.6, 125.4, 131.6, 134.5, 145.0, 145.3, 149.3 IR (ATR, cm^{-1}): 1635, 1615, 1579 ($\nu_{C=CN}$). HRMS-EI(+) (m/z): $[M]^+$ calcd for $C_{20}H_{14}N_2O_3$ 330.1004; found 330.1004. Actual charts are shown in Figures S36.

*(E)-N-{2-(4-nitrophenyl)propen-1-yl}-N-phenylbenzenamine (**11**).*[30] Although the product should be a mixture of stereoisomers, only one isomer was isolated. The reaction of **7** (693 mg, 2.00 mmol) with TMDS (537.6 mg, 4.00 mmol) was performed in the presence of **1Y** (0.5 mol%) in toluene (20 mL) at 30 °C in oil bath for 6 h. The product **11** was obtained as a bright red solid (383 mg, 1.16 mmol, 58%). Mp: 120 ~ 121 °C. ^1H NMR of **11** (400 MHz, $CDCl_3$, r.t.): δ 1.67 (s, 3H, CH=CCH_3), 6.81 (s, 1H, C*H*=CCH_3), 7.08 (t, J_{H-H} = 7.3 Hz, 2H, *p-Ph*), 7.11 (d, J_{H-H} = 8.3 Hz, 4H, *o-Ph*), 7.31 (dd, *J* = 7.3, 8.3 Hz, 4 H, *m-Ph*), 7.53 (d, J_{H-H} = 7.3 Hz, 2 H, $C_6H_4NO_2$), 8.16 (d, J_{H-H} = 7.3 Hz, 2 H, $C_6H_4NO_2$). $^{13}C\{^1H\}$ NMR of **12** (100 MHz, $CDCl_3$, r.t.): δ 16.0, 121.0, 122.8, 123.6, 123.9, 125.3, 129.5, 134.5, 145.8, 146.3, 149.2. IR (ATR, cm^{-1}): 1626, 1580 ($\nu_{C=CN}$). HRMS-EI(+) (m/z): $[M]^+$ calcd for $C_{21}H_{18}N_2O_2$ 330.1368; found 330.1364. The stereochemistry around the C=C bond was determined by

COSY and NOESY spectrum to be *E*-configuration (Figures S37 (b) and (c)). Actual charts are shown in Figures S37.

*N-[2-{4-(4'-nitrophenyl)phenyl}ethenyl]-N-phenylbenzenamine (**12**).*[30] The reaction of **8** (204 mg, 0.50 mmol) with TMDS (134.4 mg, 1.00 mmol) was performed in the presence of **1Y** (0.5 mol%) in toluene (5 mL) at 30 °C in oil bath for 6 h. The product **12** was obtained as a red solid (118 mg, 0.30 mmol, 59%). Mp: 194 ~ 195 °C. ^{1}H NMR (400 MHz, $CDCl_3$, r.t.): δ 5.62 (d, J_{H-H} = 14.2 Hz, 1H, CH=C*H*), 7.13 (d, J_{H-H} = 7.7 Hz, 4H, *o-Ph*), 7.17 (t, J_{H-H} = 7.7 Hz, 2H, *p-Ph*), 7.31 (d, J_{H-H} = 8.2 Hz, 2 H, C_6H_4-$C_6H_4NO_2$), 7.37 (dd, J_{H-H} = 7.7 Hz, 4 H, *m-Ph*), 7.51 (d, J_{H-H} = 14.2 Hz, 1H, C*H*=CH), 7.53 (d, J_{H-H} = 8.2 Hz, 2 H, C_6H_4-$C_6H_4NO_2$), 7.72 (d, J_{H-H} = 8.8 Hz, 2 H, C_6H_4-$C_6H_4NO_2$), 8.27 (d, J_{H-H} = 8.8 Hz, 2 H, C_6H_4-$C_6H_4NO_2$). ^{13}C{^{1}H} NMR (100 MHz, $CDCl_3$, r.t.): δ 107.7, 117.9, 119.8, 124.0, 124.3, 124.5, 125.1, 127.1, 127.7, 129.8, 134.8, 139.6, 145.2, 146.7. IR (ATR, cm^{-1}): 1628, 1586 ($\nu_{C=CN}$). HRMS-EI(+) (m/z): [M]$^+$ calcd for $C_{26}H_{20}N_2O_2$ 392.1525; found 392.1525. Actual charts are shown in Figures S38.

Preparation of D-π-A-π-D enamines 14 (Scheme 5).[30] In a 20 mL two-necked flask were placed the amide **13** (353 mg, 0.50 mmol), the iridium catalyst **1Y** (7.1 mg, 0.005 mmol, 0.5 mol%). The mixture was dissolved in toluene (7.0 mL), and anisole (54 μl, 0.50 mmol, as an

internal standard) and TMDS (268.8 mg, 2.00 mmol) were added. The mixture was stirred at 30 °C in oil bath for 4 h. The conversion of **13** and yields of the resulting enamine **14** were determined by ^{1}H NMR spectroscopy. After the reaction, the resulting silane residue including unreacted TMDS and the solvent were removed *in vacuo*. The obtained red viscous solid was again dissolved in pentane (10 mL), and cooled at –30 °C for 12h. The enamine **14** was obtained as red crystal (300 mg, 0.45 mmol, 89%). Mp: 227 ~ 228 °C. [CAS 2243706-34-3]. ^{1}H NMR (400 MHz, $CDCl_3$, r.t.): δ 5.70 (d, $J_{H\text{-}H}$ = 14.2 Hz, 2H, CH=C*H*), 7.15 (d, $J_{H\text{-}H}$ = 8.3 Hz, 8H, *o-Ph*), 7.16 (t, $J_{H\text{-}H}$ = 8.3 Hz, 4H, *p-Ph*), 7.37 (d, $J_{H\text{-}H}$ = 8.6 Hz, 4H, -C_6H_4-BTD-C_6H_4-), 7.37 (dd, $J_{H\text{-}H}$ = 8.3,8.3 Hz, 8H, *m-Ph*), 7.50 (d, $J_{H\text{-}H}$ = 14.2 Hz, 1H, C*H*=CH), 7.75 (s, 2H, BTD), 7.89 (d, $J_{H\text{-}H}$ = 8.6 Hz, 4H, -C_6H_4-BTD-C_6H_4-). ^{13}C{^{1}H} NMR (100 MHz, $CDCl_3$, r.t.): δ 108.7, 118.0, 121.1, 124.0, 124.2, 124.7, 127.5, 129.5, 129.5, 129.8, 134.3, 138.6, 145.4. IR (ATR, cm^{-1}): 1631, 1588 ($\nu_{C=CN}$). HRMS-EI(+) (m/z): $[M]^+$ calcd for $C_{46}H_{34}N_4S$ 674.2504; found 674.2504. Actual charts are shown in Figures S40.

UV-vis absorption and fluorescence measurements. UV-vis absorption spectra were measured on a JASCO V-650DS spectrometer (for solution) and SHIMADZU UV-3150 (for solid). Fluorescence emission spectra were measured on a JASCO FP-6500 spectrometer and HAMAMATSU C9920-02 (for quantum yield). Spectral data of UV-vis absorption and

fluorescence are described in supporting information, section 1. UV-vis absorption spectral data of all enamines and enamine-$B(C_6F_5)_3$ adducts are summarized in Tables S1 and S2, and their actual charts are shown in Figures S45~S65. Since some of the enamines and enamine-$B(C_6F_5)_3$ adducts did not exhibit strong emissions ($\Phi_{fl} < 0.01$), fluorescence spectral data for selected emissive enamines and enamine-$B(C_6F_5)_3$ adducts are listed in Tables S3 and S4. In Figures S45~S53 are shown actual charts of UV-vis spectra for non-emissive compounds, whereas absorption, fluorescence spectral charts as well as the photos are shown in Figures S54~S65.

Treatment of enamines 4k with various amount of $B(C_6F_5)_3$ (Figure 6). The reaction was performed in a nitrogen filled globe-box to avoid the contamination of moisture. Two solutions were prepared, the enamine **4k** (3.0 mg, 0.01 mmol) dissolved in $CHCl_3$ (10.0 mL) (*solution A*) and $B(C_6F_5)_3$ (5.1 mg, 0.01 mmol) dissolved in $CHCl_3$ (10.0 mL) (*solution B*). In a 20 mL vial were added the *solution A* (0.1 mL) and calculated amount of the solution *B* ($n \times 10^{-1}$ mL for n equivalent toward **4k**). The mixture was stirred at ambient temperature for 2 h. The resulting solution were diluted into 10^{-5} M by $CHCl_3$, and subjected to the measurement of UV spectra.

Treatment of enamines 4g, 4i, 4k and 4m with $B(C_6F_5)_3$ (Table 8 and Scheme 4). In a 20 mL two-necked flask were placed the enamine **4g**, **4i**, **4k** or **4m** (0.01 mmol), CH_2Cl_2 (1.0 mL) and $B(C_6F_5)_3$ (5.1 mg, 0.01 mmol). The mixture was stirred at ambient temperature for 2 h. After removal of the solvent, the resulting viscous solid was dissolved in six solvents (hexane, toluene, $CHCl_3$, or CH_2Cl_2). Each sample ($2.0 \times 10^{-4} \sim 5.0 \times 10^{-6}$ M) was subjected to the measurement of UV and FL spectra. UV and fluorescence spectra in solid states were also measured on a quartz dish. The obtained maximum absorption and fluorescence wavelengths, and their quantum yields were listed in Tables S2 and S4, and their actual spectra were also summarized in Figures S62~S65 in SI. Due to the equilibrium between the enamine and its $B(C_6F_5)_3$ adduct, two signals were visible in UV and fluorescence spectra in hexane, toluene, $CHCl_3$, and CH_2Cl_2. No adduct signals were visible when THF or DMF was used as the solvent. The above described viscous solid was dissolved in dehydrated $CDCl_3$ (0.5 mL, 2.0×10^{-2} M), which was placed in a Pyrex NMR tube, and was subjected to ^1H NMR analysis under inert gas atmosphere. A single signal due to the adduct was visible. Attempts to obtain analytically pure samples by recrystallization of the viscous solid was so far unsuccessful due to the equilibrium between the enamine and the adduct.

^{1}H NMR of **4g·B(C$_6$F$_5$)$_3$** (600 MHz, $CDCl_3$, r.t.): δ 5.54 (d, J_{H-H} = 12.8 Hz, 1H, CH=C*H*), 7.14 (d, J_{H-H} = 8.6 Hz, 4H, *o-Ph*), 7.26 (t, J_{H-H} = 8.6 Hz, 2H, *p-Ph*), 7.33 (d, J_{H-H} = 9.1 Hz, 2H, C_6H_4CN), 7.42 (dd, J_{H-H} = 8.6, 8.6 Hz, 4H, *m-Ph*), 7.64 (d, J_{H-H} = 9.1 Hz, 2H, C_6H_4CN), 7.76 (d, J_{H-H} = 12.8 Hz, 1H, C*H*=CH). Actual chart is shown in Figure S41.

^{1}H NMR of **4i·B(C$_6$F$_5$)$_3$** (600 MHz, $CDCl_3$, r.t.): δ 2.58 (s, 3H, COC*H$_3$*), 5.59 (d, J_{H-H} = 13.7 Hz, 1H, CH=C*H*), 7.15 (d, J_{H-H} = 7.8 Hz, 4H, *o-Ph*), 7.27 (d, J_{H-H} = 9.1 Hz, 2H, $C_6H_4COCH_3$), 7.28 (t, J_{H-H} = 7.8 Hz, 2H, *p-Ph*), 7.43 (dd, J_{H-H} = 7.8, 7.8 Hz, 4H, *m-Ph*), 7.87 (d, J_{H-H} = 13.7 Hz, 1H, C*H*=CH), 7.95 (d, J_{H-H} = 9.1 Hz, 2H, $C_6H_4COCH_3$). Actual chart is shown in Figure S42.

^{1}H NMR of **4k·B(C$_6$F$_5$)$_3$** (400 MHz, $CDCl_3$, r.t.): δ5.63 (d, J_{H-H} = 12.8 Hz, 1H, CH=C*H*), 7.17 (d, J_{H-H} = 8.6 Hz, 4H, *o-Ph*), 7.33 (br-d, 1H, C_6H_4CHO), 7.32 (d, J_{H-H} = 8.6 Hz, 2H, *p-Ph*), 7.37 (br-d, 1H, C_6H_4CHO), 7.45 (dd, J_{H-H} = 8.6, 8.6 Hz, 4H, *m-Ph*), 7.64 (br-d, 1H, C_6H_4CHO), 8.01 (d, J_{H-H} = 12.8 Hz, 1H, C*H*=CH), 8.14 (br-d, 1H, C_6H_4CHO), 8.64 (s, 1H, C*H*O). Actual chart is shown in Figure S43.

^{1}H NMR of **4m·B(C$_6$F$_5$)$_3$** (600 MHz, $CDCl_3$, r.t.): δ 5.70 (d, J_{H-H} = 13.7 Hz, 1H, CH=C*H*), 7.19 (d, J_{H-H} = 8.3 Hz, 4H, *o-Ph*), 7.25 (d, J_{H-H} = 8.6 Hz, 2H, $C_6H_4NO_2$), 7.36 (d, J_{H-H} = 8.3

Hz, 2H, *p-Ph*), 7.48 (dd, J_{H-H} = 8.3, 8.3 Hz, 4H, *m-Ph*), 8.06 (d, J_{H-H} = 13.7 Hz, 1H, C*H*=CH), 8.09 (d, J_{H-H} = 8.6 Hz, 2H, $C_6H_4NO_2$). Actual chart is shown in Figure S44.

DFT calculations. All of the calculations were performed using the Gaussian 09 program rev. C.[31] For optimization, B3LYP[32] functional and 6-31G**[33] basis set were selected unless otherwise noted. All stationary point structures were found to have no imaginary frequencies. For TD-DFT, B3LYP-D[34] functional and 6-311+G**[35] basis sets were used unless otherwise noted. In case of **4e** and *p*-IC_6H_4-NPh_2, SDD (Stuttgart/Dresden pseudopotentials)[36] basis set was selected for I atom. Calculated data for all compounds which were not listed in the main text are described in supporting information, section 2. Calculated energies of HOMO and LUMO with their energy gaps and simulated excitation wavelengths of S1 transition for enamines **4**, **9-12** and **14**, for the corresponding amines *p*-ZC_6H_4-NPh_2 (Z = H, F, Cl, Br, I, BTD, CN, CO_2Me, COMe, CHO, NO_2), and for enamine-$B(C_6F_5)_3$ adducts **4·B(C_6F_5)$_3$** are summarized in Tables S5~S7. The results of TD-DFT calculation for enamines **4**, **9-12** and **14**, and for enamine-$B(C_6F_5)_3$ adducts **4·B(C_6F_5)$_3$** are summarized in Tables S8 and S9, and corresponding molecular orbitals are shown in Figures S3 and S4. All cartesian coordinates (xyz), computed total energies with zero-point energy correction values and thermal correction values to gibbs free energy are listed in *2-3*.

(10) Supporting Information availability statement

The Supporting Information is available free of charge on the ACS Publications website.

Absorption and Fluorescence Spectral Data for Enamines Experimentally Obtained, Calculation Results for Enamines and Amines, and Actual charts for Amides and Enamines (.pdf).

(11) Acknowledgments

This work was supported by Integrated Research Consortium on Chemical Sciences (IRCCS), the Cooperative Research Program of "Network Joint Research Center for Materials and Devices." and JSPS KAKENHI Grant Numbers JP17K17944, JP19K05504 (A.T.), JP18H01980 and JP18K19082 (H.N.). We also appreciate supports from Prof. Katsuhiko Fujita (Kyushu Univ.) and Prof. Shin-ichiro Isobe (Kyushu Sangyo Univ.) for measurement of UV and fluorescence spectra including determination of fluorescence quantum yields.

(12) References and Endnotes.

(1) (a) Stork, G.; Brizzolara, A.; Landesman, H.; Szmuszkovicz, J.; Terrell, R. The enamine alkylation and acylation of carbonyl compounds. *J. Am. Chem. Soc.* **1963**, *85*, 207-222, DOI: 10.1021/ja00885a021. (b) Hickmott, P. W. Enamines: recent advances in synthetic, spectroscopic, mechanistic, and stereochemical aspects—I. *Tetrahedron* **1982**, *38*, 1975-2050, DOI: 10.1016/0040-4020(82)85149-1. (c) *Enamines: Synthesis, Structure, and Reactions*; 2nd ed.; Cook, A. G., Ed.; Marcel Dekker: New York, N. Y., 1987. (d) *The Chemistry of Enamines*; Rappoport, Z., Ed.; Wiley: Chichester, UK, 1994. (e) For a recent progress on enamine synthesis; Bélanger, G.; Doré, M.; Ménard, F.; Darsigny, V. Highly chemoselective formation of aldehyde enamines under very mild reaction conditions. *J. Org. Chem.* **2006**, *71*, 7481-7484, DOI: 10.1021/jo0611061.

(2) (a) For a review; Dehli, J. R.; Legros, J.; Bolm, C. Synthesis of enamines, enol ethers and related compounds by cross-coupling reactions. *Chem. Commun.* **2005**, 973-986, DOI: 10.1039/b415954c. (b) Zhang, X.; Fried, A.; Knapp, S.; Goldman, A. S. Novel synthesis of enamines by iridium-catalyzed dehydrogenation of tertiary amines. *Chem. Commun.* **2003**, 2060-2061, DOI: 10.1039/b304357f. (c) Barluenga, J.; Fernandez, M. A.; Aznar, F.; Valdes, C. Palladium-catalyzed cross-coupling reactions of amines with alkenyl bromides: a new method for the synthesis of enamines and imines. *Chem. Eur. J.* **2004**, *10*, 494-507, DOI:

10.1002/chem.200305406. (d) Venkat Reddy, C. R.; Urgaonkar, S.; Verkade, J. G. A highly effective catalyst system for the Pd-catalyzed amination of vinyl bromides and chlorides. *Org. Lett.* **2005**, *7*, 4427-4430, DOI: 10.1021/ol051612x. (e) Yan, X.; Chen, C.; Zhou, Y.; Xi, C. Copper-catalyzed electrophilic amination of alkenylzirconocenes with *O*-benzoylhydroxylamines: an efficient method for synthesis of enamines. *Org. Lett.* **2012**, *14*, 4750-4753, DOI: 10.1021/ol302004t. (f) Fukumoto, Y.; Asai, H.; Shimizu, M.; Chatani, N. Anti-Markovnikov addition of both primary and secondary amines to terminal alkynes catalyzed by the $TpRh(C_2H_4)_2/PPh_3$ system. *J. Am. Chem. Soc.* **2007**, *129*, 13792-13793, DOI: 10.1021/ja075484e.

(3) (a) Motoyama, Y.; Aoki, M.; Takaoka, N.; Aoto, R.; Nagashima, H. Highly efficient synthesis of aldenamines from carboxamides by iridium-catalyzed silane-reduction/dehydration under mild conditions. *Chem. Commun.* **2009**, 1574-1576, DOI: 10.1039/b821317h. (b) Tahara, A.; Miyamoto, Y.; Aoto, R.; Shigeta, K.; Une, Y.; Sunada, Y.; Motoyama, Y.; Nagashima, H. Catalyst design of Vaska-Type iridium complexes for highly efficient synthesis of π-conjugated enamines. *Organometallics* **2015**, *34*, 4895-4907, DOI: 10.1021/acs.organomet.5b00636. (c) Une, Y.; Tahara, A.; Miyamoto, Y.; Sunada, Y.; Nagashima, H. Iridium-PPh_3 catalysts for conversion of amides to enamines.

Organometallics **2019**, *38*, 852-862, DOI: 10.1021/acs.organomet.8b00835. (d) For a titanium-promoted conversion of amides to aldehydes via enamines, Bower, S.; Kreutzer, K. A.; Buchwald, S. L. A mild general procedure for the one-pot conversion of amides to aldehydes. *Angew. Chem. Int. Ed.* **1996**, *35*, 1515-1516, DOI: 10.1002/anie.199615151.

(4) Smith, M. B. March's Advanced Organic Chemistry: Reactions, Mechanisms, and Structure; John Wiley & Sons, Inc.: Hoboken, New Jersey, 2015.

(5) For reviews on hydrosilane reduction of amides, (a) B. Marcinec, J. G., W. Urbaniak, Z. W. Kornetka *Comprehensive handbook on hydrosilylation*; Pergamon: Oxford, 1992. (b) Larson, G. L.; Fry, J. L. *Ionic and organometallic-catalyzed organosilane reductions*; John Wiley & Sons, 2009; Vol. 81. (c) *Hydrosilylation: A Comprehensive Reviews on Recent Advances*; Marciniec, B., Ed.; Springer: Berlin, Germany, 2010. (d) Addis, D.; Das, S.; Junge, K.; Beller, M. Selective Reduction of carboxylic acid derivatives by catalytic hydrosilylation. *Angew. Chem., Int. Ed.* **2011**, *50*, 6004-6011, DOI: 10.1002/anie.201100145. (e) Nagashima, H. Efficient Transition metal-catalyzed reactions of carboxylic acid derivatives with hydrosilanes and hydrosiloxanes, afforded by catalyst design and the proximity effect of two Si-H groups. *Synlett* **2015**, *26*, 866-890, DOI: 10.1055/s-0034-1379989. (f) Sunada, Y.;

Nagashima, H. Disilametallacyclic chemistry for efficient catalysis. *Dalton Trans.* **2017**, *46*, 7644-7655, DOI: 10.1039/c7dt01275f.

(6) (a) Barbe, G.; Charette, A. B. Highly chemoselective metal-free reduction of tertiary amides. *J. Am. Chem. Soc.* **2008**, *130*, 18-19, DOI: 10.1021/ja077463q. (b) Sasakuma, H.; Motoyama, Y.; Nagashima, H. Functional group-selective poisoning of molecular catalysts: a ruthenium cluster-catalysed highly amide-selective silane reduction that does not affect ketones or esters. *Chem. Commun.* **2007**, 4916-4918, DOI: 10.1039/b711743d. (c) Das, S.; Addis, D.; Zhou, S.; Junge, K.; Beller, M. Zinc-catalyzed reduction of amides: unprecedented selectivity and functional group tolerance. *J. Am. Chem. Soc.* **2010**, *132*, 1770-1771, DOI: 10.1021/ja910083q. (d) Yumino, S.; Hashimoto, T.; Tahara, A.; Nagashima, H. Me_2S-induced highly selective reduction of aldehydes in the presence of ketones involving aldehyde-selective rate enhancement: A triruthenium cluster-catalyzed hydrosilylation. *Chem. Lett.* **2014**, *43*, 1829-1831, DOI: 10.1246/cl.140731. (e) Tinnis, F.; Volkov, A.; Slagbrand, T.; Adolfsson, H. Chemoselective reduction of tertiary amides under thermal control: Formation of either aldehydes or amines. *Angew. Chem. Int. Ed.* **2016**, *55*, 4562-4566, DOI: 10.1002/anie.201600097. (f) Mukherjee, D.; Shirase, S.; Mashima, K.; Okuda, J.

Chemoselective reduction of tertiary amides to amines catalyzed by triphenylborane. *Angew. Chem. Int. Ed.* **2016**, *55*, 13326-13329, DOI: 10.1002/anie.201605236.

(7) (a) Sinicropi, J. A.; Cowdery-Corvan, J. R.; Magin, E. H.; Borsenberger, P. M. Hole transport in vapor deposited enamines and enamine doped polymers. *Chem. Phys.* **1997**, *218*, 331-339, DOI: 10.1016/S0301-0104(97)00081-5. (b) Matoliukstyte, A.; Burbulis, E.; Grazulevicius, J. V.; Gaidelis, V.; Jankauskas, V. Carbazole-containing enamines as charge transport materials for electrophotography. *Synth. Met.* **2008**, *158*, 462-467, DOI: 10.1016/j.synthmet.2008.03.020. (c) Paspirgelyte, R.; Grazulevicius, J. V.; Grigalevicius, S.; Jankauskas, V. Phenoxazine and N-phenyl-1-naphtylamine-based enamines as hole-transporting glass-forming materials. *Synth. Met.* **2009**, *159*, 1014-1018, DOI: 10.1016/j.synthmet.2009.01.015.

(8) (a) Dou, L.; Liu, Y.; Hong, Z.; Li, G.; Yang, Y. Low-bandgap near-IR conjugated polymers/molecules for organic electronics. *Chem Rev* **2015**, *115*, 12633-12665, DOI: 10.1021/acs.chemrev.5b00165. (b) For a review on semiconducting polymers, Osaka, I. Semiconducting polymers based on electron-deficient π-building units. *Polymer J.* **2014**, *47*, 18-25, DOI: 10.1038/pj.2014.90. (c) For applications to sensors; Ramachandran, E.; Vandarkuzhali, S. A. A.; Sivaraman, G.; Dhamodharan, R. Phenothiazine based donor-

acceptor compounds with solid-state emission in the yellow to NIR region and their highly selective and sensitive detection of cyanide ion in ppb level. *Chem. Eur. J.* **2018**, *24*, 11042-11050, DOI: 10.1002/chem.201800216. (d) Applications to data storage; Shang, Y.; Wen, Y.; Li, S.; Du, S.; He, X.; Cai, L.; Li, Y.; Yang, L.; Gao, H.; Song, Y. A triphenylamine-containing donor-acceptor molecule for stable, reversible, ultrahigh density data storage. *J. Am. Chem. Soc.* **2007**, *129*, 11674-11675, DOI: 10.1021/ja074226e. (e) Akimiya, K.; Osaka, I.; Nakano, M. π-Building blocks for organic electronics: Revaluation of "Inductive" and "Resonance" effects of π-electron deficient units. *Chem. Mater.* **2013**, *26*, 587-593, DOI: 10.1021/cm4021063. (f) Review; Liu, C.; Wang, K.; Gong, X.; Heeger, A. J. Low bandgap semiconducting polymers for polymeric photovoltaics. *Chem. Soc. Rev.* **2016**, *45*, 4825-4846, DOI: 10.1039/C5CS00650C.

(9) Iranpoor, N.; Firouzabadi, H.; Azadi, R. Diphenylphosphinite ionic liquid (IL-$OPPh_2$): A solvent and ligand for palladium-catalyzed silylation and dehalogenation reaction of aryl halides with triethylsilane. *J. Organomet. Chem.* **2010**, *695*, 887-890, DOI: 10.1016/j.jorganchem.2010.01.001.

(10) Labinger, J. A.; Osborn, J. A. Mechanistic studies of oxidative addition to low-valent metal complexes. Stereochemistry at carbon in addition of alkyl halides to iridium(I). *Inorg. Chem.* **1980**, *19*, 3230-3236, DOI: 10.1021/ic50213a006.

(11) Zhang, M.; Tsao, H. N.; Pisula, W.; Yang, C.; Mishra, A. K.; Mullen, K. Field-effect transistors based on a benzothiadiazole-cyclopentadithiophene copolymer. *J. Am. Chem. Soc.* **2007**, *129*, 3472-3473, DOI: 10.1021/ja0683537. (b) Dhanabalan, A.; van Duren, J. K. J.; van Hal, P. A.; van Dongen, J. L. J.; Janssen, R. A. J. Synthesis and characterization of a low bandgap conjugated polymer for bulk heterojunction photovoltaic cells. *Adv. Funct. Mater.* **2001**, *11*, 255-262, DOI: 10.1002/1616-3028(200108)11:4<255::AID-ADFM255>3.0.CO;2-I (c) Jiang, D.; Chen, S.; Xue, Z.; Li, Y.; Liu, H.; Yang, W.; Li, Y. Donor–acceptor molecules based on benzothiadiazole: Synthesis, X-ray crystal structures, linear and third-order nonlinear optical properties. *Dyes Pigm.* **2016**, *125*, 100-105, DOI: 10.1016/j.dyepig.2015.10.014.

(12) For reviews; (a) Blaser, H.-U.; Steiner, H.; Studer, M. Selective catalytic hydrogenation of functionalized nitroarenes: An Update. *ChemCatChem* **2009**, *1*, 210-221, DOI: 10.1002/cctc.200900129. (b) Lara, P.; Philippot, K. The hydrogenation of nitroarenes mediated by platinum nanoparticles: an overview. *Catal. Sci. Technol.* **2014**, *4*, 2445-2465,

DOI: 10.1039/C4CY00111G. (c) Song, J.; Huang, Z.-F.; Pan, L.; Li, K.; Zhang, X.; Wang, L.; Zou, J.-J. Review on selective hydrogenation of nitroarene by catalytic, photocatalytic and electrocatalytic reactions. *Appl. Catal. B* **2018**, *227*, 386-408, DOI: 10.1016/j.apcatb.2018.01.052.

(13) (a) Lipowitz, J.; Bowman, S. A. Use of polymethylhydrosiloxane as a selective, neutral reducing agent for aldehydes, ketones, olefins, and aromatic nitro compounds. *J. Org. Chem.* **1973**, *38*, 162-165, DOI: 10.1021/jo00941a039. (b) Rahaim, R. J., Jr.; Maleczka, R. E., Jr. Pd-catalyzed silicon hydride reductions of aromatic and aliphatic nitro groups. *Org. Lett.* **2005**, *7*, 5087-5090, DOI: 10.1021/ol052120n. (c) Sunada, Y.; Kawakami, H.; Imaoka, T.; Motoyama, Y.; Nagashima, H. Hydrosilane reduction of tertiary carboxamides by iron carbonyl catalysts. *Angew. Chem. Int. Ed.* **2009**, *48*, 9511-9514, DOI: 10.1002/anie.200905025.

(14) Kornblum, N.; Fishbein, L. The reduction of optically active 2-nitroöctane and α-phenylnitroethane. *J. Am. Chem. Soc.* **1955**, *77*, 6266-6269, DOI: 10.1021/ja01628a063.

(15) (a) Dreeskamp, H.; Koch, E.; Zander, M. Fluorescence quenching of polycyclic aromatic-hydrocarbons by nitromethane. *Z. Naturforsch.* **1975**, *30 A*, 1311-1314, DOI: 10.1515/zna-1975-1017. (b) Farztdinov, V. M.; Schanz, R.; Kovalenko, S. A.; Ernsting, N.

P. Relaxation of optically excited *p*-nitroaniline: semiempirical quantum-chemical calculations compared to femtosecond experimental results. *J. Phys. Chem. A* **2000**, *104*, 11486-11496, DOI: 10.1021/jp001690w. (c) Arce, R.; Pino, E. F.; Valle, C.; Agreda, J. Photophysics and photochemistry of 1-nitropyrene. *J. Phys. Chem. A* **2008**, *112*, 10294-10304, DOI: 10.1021/jp803051x. (d) Collado-Fregoso, E.; Zugazagoitia, J. S.; Plaza-Medina, E. F.; Peon, J. Excited-state dynamics of nitrated push-pull molecules: the importance of the relative energy of the singlet and triplet manifolds. *J. Phys. Chem. A* **2009**, *113*, 13498-13508, DOI: 10.1021/jp905379y.

(16) For discussion on the intramolecular fluorescence quenching, see; (a) Munkholm, C.; Parkinson, D. R.; Walt, D. R. Intramolecular fluorescence self-quenching of fluoresceinamine. *J. Am. Chem. Soc.* **1990**, *112*, 2608-2612, DOI: 10.1021/ja00163a021. (b) Ueno, T.; Urano, Y.; Kojima, H.; Nagano, T. Mechanism-based molecular design of highly selective fluorescence probes for nitrative stress. *J. Am. Chem. Soc.* **2006**, *128*, 10640-10641, DOI: 10.1021/ja061972v.

(17) (a) Kotaka, H.; Konishi, G.-i.; Mizuno, K. Synthesis and photoluminescence properties of π-extended fluorene derivatives: the first example of a fluorescent solvatochromic nitro-group-containing dye with a high fluorescence quantum yield.

Tetrahedron Lett. **2010**, *51*, 181-184, DOI: 10.1016/j.tetlet.2009.10.118. (b) Hachiya, S.; Asai, K.; Konishi, G.-i. Unique solvent-dependent fluorescence of nitro-group-containing naphthalene derivatives with weak donor–strong acceptor system. *Tetrahedron Lett.* **2013**, *54*, 1839-1841, DOI: 10.1016/j.tetlet.2013.01.096. (c) Hachiya, S.; Asai, K.; Konishi, G.-i. Environment-responsive multicolor fluorescent dyes based on nitrophenyl or nitrophenylethynyl oligothiophene derivatives: correlation between fluorescence and π-conjugation length. *Tetrahedron Lett.* **2013**, *54*, 3317-3320, DOI: 10.1016/j.tetlet.2013.03.054.

(18) (a) Wu, J.-H.; Chen, W.-C.; Liou, G.-S. Triphenylamine-based luminogens and fluorescent polyimides: effects of functional groups and substituents on photophysical behaviors. *Polym. Chem.* **2016**, *7*, 1569-1576, DOI: 10.1039/C5PY01939G (See, page 30 in SI). (b) Johnsen, M.; Paterson, M. J.; Arnbjerg, J.; Christiansen, O.; Nielsen, C. B.; Jorgensen, M.; Ogilby, P. R. Effects of conjugation length and resonance enhancement on two-photon absorption in phenylene-vinylene oligomers. *Phys. Chem. Chem. Phys.* **2008**, *10*, 1177-1191, DOI: 10.1039/B715441K. (c) Zhao, W.; He, Z.; Peng, Q.; Lam, J. W. Y.; Ma, H.; Qiu, Z.; Chen, Y.; Zhao, Z.; Shuai, Z.; Dong, Y.; Tang, B. Z. Highly sensitive switching of solid-state

luminescence by controlling intersystem crossing. *Nat. Commun.* **2018**, *9*, 3044, DOI: 10.1038/s41467-018-05476-y.

(19) For a review on optical properties of D-π-A molecules; Meier, H. Conjugated oligomers with terminal donor-acceptor substitution. *Angew. Chem. Int. Ed.* **2005**, *44*, 2482-2506, DOI: 10.1002/anie.200461146.

(20) (a) For a review; Reichardt, C. Solvatochromic dyes as solvent polarity indicators. *Chem. Rev.* **1994**, *94*, 2319-2358, DOI: 10.1021/cr00032a005. (b) Marini, A.; Munoz-Losa, A.; Biancardi, A.; Mennucci, B. What is solvatochromism? *J. Phys. Chem. B* **2010**, *114*, 17128-17135, DOI: 10.1021/jp1097487.

(21) Mizuno and coworkers found emissive nitro compounds, and the reason why nitro compounds did not show fluorescence in polar solvents was ascribed to Twisted Intramolecular Charge Transfer (TICT). See, ref. 17a and the following references: For a review, Sasaki, S.; Drummen, G. P. C.; Konishi, G.-i. Recent advances in twisted intramolecular charge transfer (TICT) fluorescence and related phenomena in materials chemistry. *J. Mater. Chem. C* **2016**, *4*, 2731-2743, DOI: 10.1039/C5TC03933A. (b) Yang, J.-S.; Lin, C.-J. Fate of photoexcited trans-aminostilbenes. *J. Photochem. Photobiol. A* **2015**, *312*, 107-120, DOI: 10.1016/j.jphotochem.2015.05.031.

(22) Balter, A.; Nowak, W.; Pawełkiewicz, W.; Kowalczyk, A. Some remarks on the interpretation of the spectral properties of prodan. *Chem. Phys. Lett.* **1988**, *143*, 565-570, DOI: 10.1016/0009-2614(88)87067-2.

(23) Kucherak, O. A.; Didier, P.; Mély, Y.; Klymchenko, A. S. Fluorene Analogues of Prodan with Superior Fluorescence Brightness and Solvatochromism. *J. Phys. Chem. Lett.* **2010**, *1*, 616-620, DOI: 10.1021/jz9003685.

(24) (a) Nishida, T.; Fukazawa, A.; Yamaguchi, E.; Oshima, H.; Yamaguchi, S.; Kanai, M.; Kuninobu, Y. Synthesis of pyridine N-oxide-BF_2CF_3 complexes and their fluorescence properties. *Chem. Asian J.* **2014**, *9*, 1026-1030, DOI: 10.1002/asia.201301688. (b) Hansmann, M. M.; Lopez-Andarias, A.; Rettenmeier, E.; Egler-Lucas, C.; Rominger, F.; Hashmi, A. S.; Romero-Nieto, C. $B(C_6F_5)_3$: A Lewis acid that brings the light to the solid state. *Angew. Chem. Int. Ed.* **2016**, *55*, 1196-1199, DOI: 10.1002/anie.201508461. (c) Murai, T.; Yamaguchi, K.; Hayano, T.; Maruyama, T.; Kawai, K.; Kawakami, H.; Yashita, A. Synthesis and photophysical properties of 5-*N*-arylamino-4-methylthiazoles obtained from direct C–H arylations and Buchwald–Hartwig aminations of 4-methylthiazole. *Organometallics* **2017**, *36*, 2552-2558, DOI: 10.1021/acs.organomet.7b00128. (d) Yamakawa, T.; Yoshigoe, Y.; Wang, Z.; Kanai, M.; Kuninobu, Y. Preparation of solid-state

luminescent materials by complexation between π-conjugated molecules and activators. *Chem. Lett.* **2018**, *47*, 1391-1394, DOI: 10.1246/cl.180735.

(25) Selected examples for applications of the Ir / TMDS catalysis system into further transformations.; (a) Gregory, A. W.; Chambers, A.; Hawkins, A.; Jakubec, P.; Dixon, D. J. Iridium-catalyzed reductive nitro-Mannich cyclization. *Chem. Eur. J.* **2015**, *21*, 111-114, DOI: 10.1002/chem.201405256. (b) Nakajima, M.; Sato, T.; Chida, N. Iridium-catalyzed chemoselective reductive nucleophilic addition to *N*-methoxyamides. *Org. Lett.* **2015**, *17*, 1696-9, 10.1021/acs.orglett.5b00664. (c) Huang, P. Q.; Ou, W.; Han, F. Chemoselective reductive alkynylation of tertiary amides by Ir and Cu(I) bis-metal sequential catalysis. *Chem. Commun.* **2016**, *52*, 11967-11970, 10.1039/c6cc05318a. (d) Gabriel, P.; Gregory, A. W.; Dixon, D. J. Iridium-Catalyzed Aza-Spirocyclization of Indole-Tethered Amides: An Interrupted Pictet−Spengler Reaction, *Org. Lett.* **2019**, *21*, 6658-6662, DOI: 10.1021/acs.orglett.9b02194. (e) Yamamoto, S.; Komiya, Y.; Kobayashi, A.; Minamikawa, R.; Oishi, T.; Sato, T.; Chida, N. Asymmetric Total Synthesis of Fasicularin by Chiral *N*-Alkoxyamide Strategy. *Org. Lett.* **2019**, *21*, 1868-1871, 10.1021/acs.orglett.9b00478. (f) Yang, Z.-P.; Lu, G.-S.; Ye, J.-L.; Huang, P. -Q. Ir-catalyzed chemoselective reduction of β-

amido esters: A versatile approach to β-enamino esters. *Tetrahedron* **2019**, *75*, 1624-1631, 10.1016/j.tet.2018.12.024, and references cited therein.

(26) Selected examples for triarylamine synthesis by cross-coupling reactions; (a) Yamamoto, T.; Nishiyama, M.; Koie, Y. Palladium-catalyzed synthesis of triarylamines from aryl halides and diarylamines. *Tetrahedron Lett.* **1998**, *39*, 2367-2370, DOI: 10.1016/S0040-4039(98)00202-0. (b) Goodbrand, H. B.; Hu, N.-X. Ligand-Accelerated Catalysis of the Ullmann Condensation: Application to Hole Conducting Triarylamines. *J. Org. Chem.* **1999**, *64*, 670-674, DOI: 10.1021/JO981804O. (c) Harris, M. C.; Buchwald, S. L. One-Pot Synthesis of Unsymmetrical Triarylamines from Aniline Precursors. *J. Org. Chem.* **2000**, *65*, 5327-5333, DOI: 10.1021/jo000674s. (d) Hooper, M. W.; Utsunomiya, M.; Hartwig, J. F. Scope and mechanism of palladium-catalyzed amination of five-membered heterocyclic halides. *J. Org. Chem.* **2003**, *68*, 2861-2873, DOI: 10.1021/jo0266339. (e) Hatakeyama, T.; Imayoshi, R.; Yoshimoto, Y.; Ghorai, S. K.; Jin, M.; Takaya, H.; Norisuye, K.; Sohrin, Y.; Nakamura, M. Iron-catalyzed aromatic amination for nonsymmetrical triarylamine synthesis. *J. Am. Chem. Soc.* **2012**, *134*, 20262-20265, DOI: 10.1021/ja309845k, and references cited therein.

(27) Hama, T.; Culkin, D. A.; Hartwig, J. F. Palladium-catalyzed intermolecular alpha-arylation of zinc amide enolates under mild conditions. *J. Am. Chem. Soc.* **2006**, *128*, 4976-4985, DOI: 10.1021/ja056076i.

(28) Schumann, J.; Kanitz, A.; Hartmann, H. Synthesis and Characterization of Some Heterocyclic Analogues of *N*,*N*′-Perarylated Phenylene-1,4-diamines and Benzidines as a New Class of Hole Transport Materials. *Synthesis* **2002**, *9*, 1268-1276. DOI: 10.1055/s-2002-32531.

(29) Wagner, G.; Eppner, B. Synthesis of 4-amidinophenylacetic acid 4-amidinophenoxyacetic amides. *Pharmazie* **1981**, *36*, 323-326, ISSN: 0031-7144.

(30) Nagashima, H.; Tahara, A.; Kitahara, I.; Kuninobu Y.; Enamine compound and use thereof as a donor-acceptor type compound. PCT / 2018-JP8116.

(31). H Frisch, M. J.; Trucks, G. W.; Schlegel, H. B.; Scuseria, G. E.; Robb, M. A.; Cheeseman, J. R.; Scalmani, G.; Barone, V.; Mennucci, B.; Petersson, G. A.; Nakatsuji, H.; Caricato, M.; Li, X.; Hratchian, H. P.; Izmaylov, A. F.; Bloino, J.; Zheng, G.; Sonnenberg, J. L.; Hada, M.; Ehara, M.; Toyota, K.; Fukuda, R.; Hasegawa, J.; Ishida, M.; Nakajima, T.; Honda, Y.; Kitao, O.; Nakai, H.; Vreven, T.; Montgomery, J. A., Jr.; Peralta, J. E.; Ogliaro, F.; Bearpark, M.; Heyd, J. J.; Brothers, E.; Kudin, K. N.; Staroverov, V. N.; Keith, T.;

Kobayashi, R.; Normand, J.; Raghavachari, K.; Rendell, A.; Burant, J. C.; Iyengar, S. S.; Tomasi, J.; Cossi, M.; Rega, N.; Millam, J. M.; Klene, M.; Knox, J. E.; Cross, J. B.; Bakken, V.; Adamo, C.; Jaramillo, J.; Gomperts, R.; Stratmann, R. E.; Yazyev, O.; Austin, A. J.; Cammi, R.; Pomelli, C.; Ochterski, J. W.; Martin, R. L.; Morokuma, K.; Zakrzewski, V. G.; Voth, G. A.; Salvador, P.; Dannenberg, J. J.; Dapprich, S.; Daniels, A. D.; Farkas, O.; Foresman, J. B.; Ortiz, J. V.; Cioslowski, J.; Fox, D. J. *Gaussian 09, Revision C.01;* Gaussian, Inc., Wallingford, CT, 2010.

(32) (a) Becke, A. D. Density-functional exchange-energy approximation with correct asymptotic behavior. *Phys. Rev. A* **1988**, *38*, 3098−3100, ISSN: 0556-2791. (b) Becke, A. D. Density-functional thermochemistry. III. The role of exact exchange. *J. Chem. Phys.* **1993**, *98*, 5648-5652, DOI: 10.1063/1.464913. (c) Lee, C.; Yang, W.; Parr, R. G. Development of the Colle-Salvetti correlation-energy formula into a functional of the electron density. *Phys. Rev. B* **1988**, *37*, 785-789, DOI: 10.1103/PhysRevB.37.785.

(33) (a) Gordon, M. S. The isomers of silacyclopropane. *Chem. Phys. Lett.* **1980**, *76*, 163-168, DOI: 10.1016/0009-2614(80)80628-2. (b) Harihara, Pc; Pople, J. A. Accuracy of AH_n equilibrium geometries by single determinant molecular orbital theory. *Mol. Phys.* **1974**, *27*, 209-214, DOI: 10.1080/00268977400100171. (c) Hariharan, P. C.; Pople, J. A. The influence

of polarization functions on molecular orbital hydrogenation energies. *Theor. Chim. Acta* **1973**, *28*, 213-222, DOI: 10.1007/BF00533485. (d) Hehre, W. J.; Ditchfield, R.; Pople, J. A. Self-Consistent molecular orbital methods. XII. Further extensions of Gaussian-type basis sets for use in molecular orbital studies of organic molecules. *J. Chem. Phys.* **1972**, *56*, 2257-2261, DOI: 10.1063/1.1677527. (e) Ditchfield, R.; Hehre, W. J.; Pople, J. A. Self-consistent molecular-orbital methods. IX. An extended Gaussian-type basis for molecular-orbital studies of organic molecules. *J. Chem. Phys.* **1971**, *54*, 724-728, DOI: 10.1063/1.1674902.

(34) (a) Stephens, P. J.; Devlin, F. J.; Chabalowski, C. F.; Frisch, M. J. Ab Initio calculation of vibrational absorption and circular dichroism spectra using density functional force fields. *J. Phys. Chem.* **1994**, *98*, 11623-11627, DOI: 10.1021/j100096a001. (b) Grimme, S. Semiempirical GGA-type density functional constructed with a long-range dispersion correction. *J. Comput. Chem.* **2006**, *27*, 1787-1799, DOI: 10.1002/jcc.20495.

(35) (a) Krishnan, R.; Binkley, J. S.; Seeger, R.; Pople, J. A. Self-consistent molecular orbital methods. XX. A basis set for correlated wave functions. *J. Chem. Phys.* **1980**, *72*, 650-654, DOI: 10.1063/1.438955. (b) McLean, A. D.; Chandler, G. S. Contracted Gaussian basis sets for molecular calculations. I. Second row atoms, Z=11–18. *J. Chem. Phys.* **1980**, *72*, 5639-5648, DOI: 10.1063/1.438980. (c) Clark, T.; Chandrasekhar, J.; Spitznagel, G. W.;

Schleyer, P. V. R. Efficient diffuse function-augmented basis sets for anion calculations. III. The 3-21+G basis set for first-row elements, Li-F. *J. Comput. Chem.* **1983**, *4*, 294-301, DOI: 10.1002/jcc.540040303.

(36) Andrae, D.; Häußermann, U.; Dolg, M.; Stoll, H.; Preuß, H. Energy-adjusted *ab initio* pseudopotentials for the second and third row transition elements. *Theor. Chim. Acta* **1990**, *77*, 123-141, DOI: 10.1007/BF01114537.